이학석사 학위논문

염생식물 비쑥(*Artemisia scoparia*)으로부터 생리활성물질 분리 및 구조결정

Isolation and Structure Determination of Bioactive Compounds from the halophyte *Artemisia scoparia*

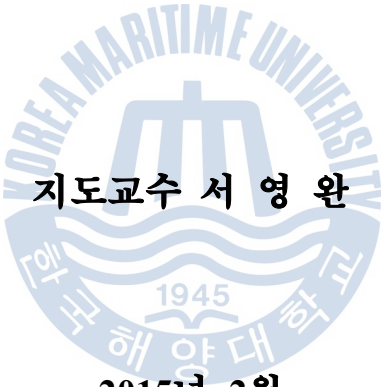

지도교수 서 영 완

2015년 2월

해 양 과 학 기 술 전 문 대 학 원

해양과학기술융합학과

김 다 슬

본 논문을 김다슬의 이학석사 학위논문으로 인준함.

위원장 임 선 영 (인)

위 원 조 성 환 (인)

위 원 서 영 완 (인)

2014년 12월 2일

한국해양대학교 해양과학기술전문대학원

Content

List of Schemes

List of Tables

List of Figures

List of Abbreviations

BHA	: butylated hydroxyanisole
BHT	: butylated hydroxytoluene
c	: concentration
CD_3OD	: deuterium methanol
CH_2Cl_2	: dichloromethane (methylene chloride)
^{13}C NMR	: carbon 13 nuclear magnetic resonance
COSY	: homonuclear correlation spectroscopy
DEPT	: distortionless enhancement by polarization transfer
DPPH	: 1,1-diphenyl-2-picryl-hydrazyl
EtOAc	: ethyl acetate
H_2O	: water
^1H NMR	: proton nuclear magnetic resonance
HMBC	: heteronuclear multiple-bond connectivity
HMQC	: heteronuclear multiple-quantum connectivity
HRFAB	: high resolution fast atom bombardment
Hz	: herz (sec^{-1})
IR	: Infrared
LRFAB	: low resolution fast atom bombardment
MeOH	: methanol
MS	: mass spectroscopy
n-BuOH	: normal-butanol
NO·	: nitric oxide radical
NOESY	: nuclear overhauser enhancement spectroscopy
$\cdot O_2^-$	: superoxide anion radical
·OH	: hydroxyl radical
$ONOO^-$	: peroxynitrite
RNS	: reactive nitrogen species
ROS	: reactive oxygen species
RP	: reverse phase
S	: substrate
SiO_2	: silica gel
TLC	: thin layer chromatography
UV	: ultraviolet
υ_{max}	: maximal velocity

염생식물 비쑥(*Artemisia scoparia*)으로부터 생리활성물질 분리 및 구조결정

Da Seul Kim

Department of Convergence Study
Ocean Science and Technology School

Abstract

염생습지에 자생하는 염생식물은 육상식물과 달리 계절과 조석의 영향으로 토양의 염분도가 극단적으로 바뀌는 환경에 자생하고 있다. 따라서 이러한 특이한 환경에 서식하는 염생식물은 육상식물과는 다른 이차대사산물을 생성시킬 가능성이 높다고 여겨진다. 또한 염생습지의 높은 염분성분은 산화환경을 야기시켜 활성산소종을 빈번히 발생시키기 때문에 염생식물들은 이러한 활성산소종을 제거하기 위한 강력한 항산화기작을 가지고 있는 것으로 알려져 있어 흥미있는 항산화물질의 존재가능성도 매우 높다고 할 수 있다.

자연으로부터 새로운 생리활성물질을 찾기 위한 노력으로 우리나라 서해안 염생습지에 서식하는 비쑥을 채집하여 조추출물을 제조한 후에 HT1080 세포내에 생성되는 활성산소종(ROS)에 대한 항산화 활성을 측정한 결과 유의적인 항산화활성이 있음을 확인하였다. 따라서 본 연구에서는 비쑥의 조추출물을 용매극성에 따라 *n*-hexane, 85% aq.MeOH, *n*-BuOH, H_2O 층으로 분획한 후 각각의 용매분획에 대한 항산화활성과 항암활성을 측정하였으며 또한 각 분획으로부터 이차 대사물질들을 분리하였다.

DPPH radical 소거활성실험에서는 *n*-BuOH 분획층이 가장 높은 항산화 효과를 보여 주었다. 세포내에 생성된 ROS의 소거와 DNA 산화 억제 실험에서는 85% aq.MeOH과 *n*-BuOH 분획층이 가장 높은 억제율을 보였다. 그리고 authentic $ONOO^-$와 SIN-1에서 유도된 $ONOO^-$의 소거 활성에서는 85% aq.MeOH 분획층이 가장 높은 소거활성을 보여 주었다.

한편 각 용매 분획물의 인체 암세포들 (HT1080, AGS, HT-29 및 MCF-7)에 대한 증식억제 실험에서는 85% aq.MeOH 분획물이 모든 암세포들에 대해 농도 의존적으로 좋은 암세포 성장 억제 효과를 나타내었고, *n*-hexane 분획물도 MCF-7를 제외한 나머지 암세포에 대해서 좋은 성장 억제 효과를 나타내었다.

이러한 생리활성을 보인 유기 용매 분획물에서 2차 대사물질들의 분리를 시도하여 *n*-hexane 분획물에서 α-Amyrin (**1**), α-Fernenol (**2**), *n*-BuOH에서 3,5-dicaffeoyl-*epi*-quinic acid (**3**)을 분리하였으며 85% aq.MeOH 분획물에서 새로운 화합물인 1-(3-acetyl-4-hydroxyphenyl)-3-hydroxy-3-methyl-1-butanone (**4**)을 분리하였다.

KEY WORDS: *Artemisia scoparia* 비쑥; Antioxidant activity 항산화활성; α-fernenol; α-amyrin; 3,5-dicaffeoyl-*epi*-quinic acid; 1-(3-acetyl-4-hydroxyphenyl)-3-hydroxy-3-methyl-1-butanone

1. Introduction

Natural substances have been actively used in the development of drugs; over 60% of the drugs currently used in the treatment of diseases are prepared from these substances. However, because of the great increase in drug resistance, new drugs to overcome the resistance must be developed. This prompts us to have a focus on isolation of the new natural products. Recent studies have shown that halophytes have a potential for drug development (김응서, 2012).

South Korea, surrounded by the sea on three sides, has a well-developed halophyte habitat. Halophytes grow naturally in intertidal areas, displaying vegetation formed by the regular effects of seawater. A marine system with a high variability in physical parameters such as temperature, salinity, or radiation can be considered to be an extreme environment. Intertidal regions such as tidal flats and salt marshes are subjected to these types of environmental extremes on a daily, seasonal, and annual basis. Organisms that exist in these environments have to acclimatize by developing specific stress adaptation responses. In many plant species, this often includes the synthesis of unusual secondary metabolites

Salt marshes are classified into low tide and high tide marshes. Colonies of *Suaeda japonica*, *Suaeda maritima* (L.) Dumort, and *Aster tripolium* L. are observed in low intertidal region (topographically low and frequently flooded by the tide. On the other hand, colonies of *Artemisia scoparia* Wald. et Kitaib, *Carex scabrifolia* Steud, and reeds are found in high tide marshes (topographically high and rarely affected by the tide (이우철, 1996). The soil

in intertidal regions is rich in salt; in addition, these areas attract the colonization of various species and have abundant quantities of nutrient salts and energy, which result in high productivity.

As mentioned above, halophytes that grow under high-salt stress will require a metabolic pathway different from those required for terrestrial plants in order to be adapted to this environment. Therefore, these species are likely to contain different secondary metabolites, compared to terrestrial plants. Based on this assumption, the halophytes were collected and screened for antioxidant and antiinflammatory capacity. These results revealed that *Artemisia scoparia* Wald. et Kitaib had the significant antioxidant and antiinflammatory effects; therefore, this species was selected and examined in this study.

The Illustrated Handbook of Flora and Fauna of Korea identifies *Artemisia scoparia* Wald. et Kitaib to be a herbaceous perennial plant that grows naturally in coastal sandy soil. This plant is classified into the genus *Artemisia*, family *Compositae*, and order Asterales. It is widely distributed in Asia and Europe, and is known to grow in the Jeju-do, Geyongggi-do, Gangwon-do, and the Northern and Southern Hamgyeong provinces in Korea. It has a straight purple stem, with a height between 40 and 100 cm, many branches on the top, and a vertically deep wrinkle. Its stem leaves have an oval shape and grow alternately. These bipinnate or tripinnate leaves are 3 to 5 cm in length and 2 to 3 cm in width. The lobed leaves are as thin as a thread, and the leaf size decreases closer to the top of the plant. It has yellowish brown capitate flowers, which are sized at approximately 1 mm (diameter) when blooming in a conical inflorescence form between August and September. Folk remedies have indicated that *Artemisia scoparia* Wald. et Kitaib can be effectively used against various infections, diuresis, neurasthenia, and headache. Particularly, it has been frequently used in the treatment of female illnesses, such as postnatal melena and uterine bleeding.

This plant is believed to possess cytotoxic (Choi, E., 2013), antioxidant (Yoon W. J., 2006), and antiinflammatory effects (Rabe S.Z.T., 2011). Furthermore, recent studies have revealed that extract of this plant prevents the activation of *Streptococcus mutans*, a bacterium belonging to the *Mutans streptococci* group that causes dental caries (Jung-Ah Seo, 2009), reduce fatty liver-related diseases (Wang Z.Q., 2013), and alleviate fever and pain (Habib M., 2013). Moreover, scopariachromane, a chromane-series substance (Tadahiro Yahagi, 2014), and scoparal, an aromatic substance (Muhammad Shaiq Ali, 2008), have been isolated from this plant. The secondary metablites isolated from this plant thus far are listed in Figure 1.

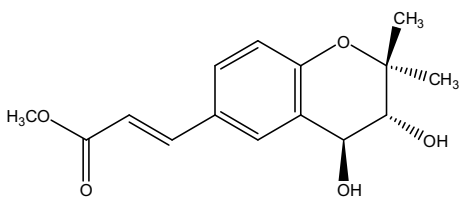

(1) Scopariachromane

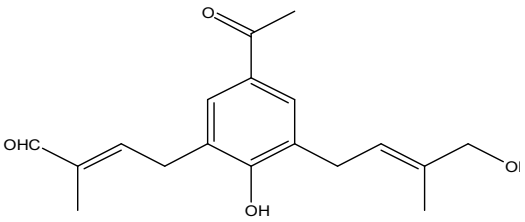

(2) Scoparal

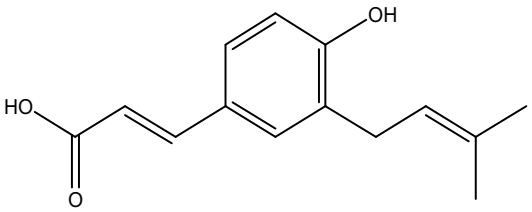

(3)

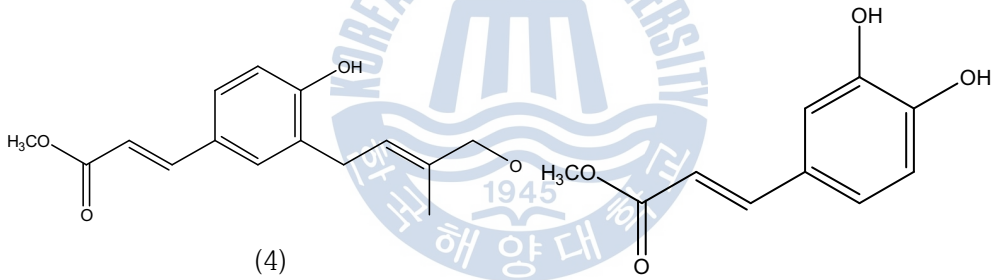

(4)

(5)

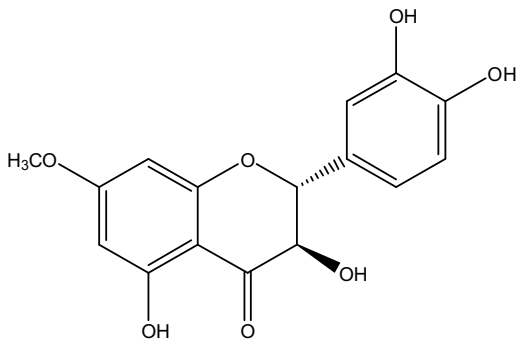

(6)

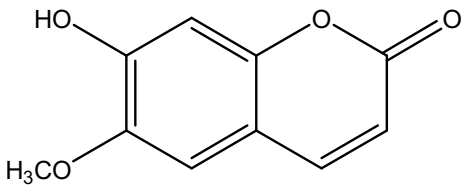

(7)

Figure 1. Compounds isolated from *Artemisia scoparia*.

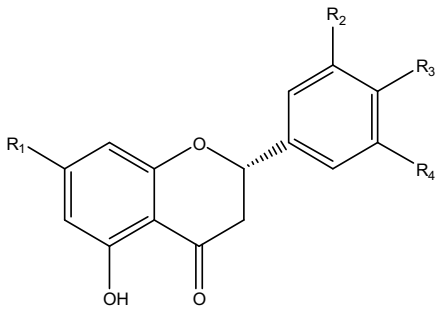

(8) R1 = OCH3, R2 = H, R3 = OH, R4 = H
(9) R1 = OH, R2 = H, R3 = OH, R4 = H
(10) R1 = OCH3, R2 = OH, R3 = H, R4 = OH
(11) R1 = OH, R2 = OH, R3 = H, R4 = OH
(12) R1 = OH, R2 = OH, R3 = OH, R4 = H

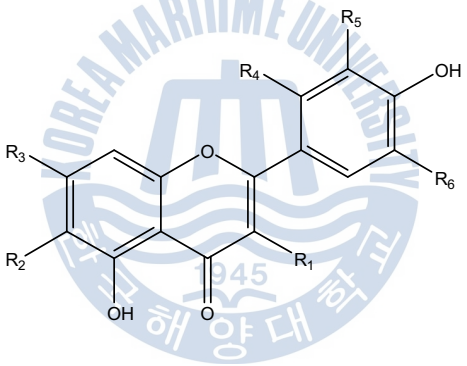

(13) R1 = H, R2 = OCH3, R3 = OCH3, R4 = H, R5 = OCH3, R6 = H
(14) R1 = H, R2 = OCH3, R3 = OCH3, R4 = H, R5 = OH, R6 = H (Cirsiliol)
(15) R1 = H, R2 = OCH3, R3 = OH, R4 = H, R5 = OCH3, R6 = H (Jaceosidin)
(16) R1 = H, R2 = OCH3, R3 = OH, R4 = OH, R5 = H, R6 = OCH3
(17) R1 = OCH3, R2 = OCH3, R3 = OH, R4 = H, R5 = OH, R6 = H
(18) R1 = O-β-D-Gal, R2 = H, R3 = OH, R4 = H, R5 = OH, R6 = H

Figure 1. (continued)

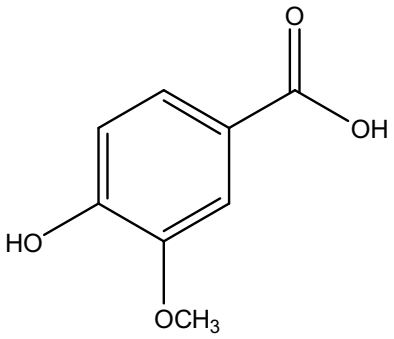

(19)

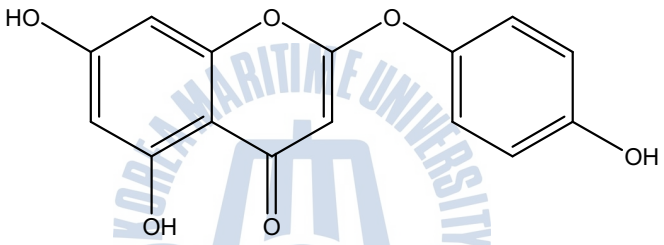

(20)

Figure 1. (continued)

2. Materials and Methods

2.1 Plant Material

Whole plants of *Artemisia scoparia* (Figure 2) were collected by hand in September, 2007 at Donggumdo tidal flat of Ganghwado, South Korea. The shade-dried materials of *Artemisia scoparia* was kept in -25 ℃ until chemically investigated.

Figure 2. Photographs of *Artemisia scoparia*.

2.2 General Experimental Procedure

NMR spectra were recorded in CD_3OD on a Varian Mercury 300 spectrometer. ^1H and ^{13}C NMR spectra were measured using standard Varian pulse sequence programs at 300 MHz and 75 MHz, respectively. All chemical shifts were recorded with respect to internal Me_4Si or residual CD_3OD peaks. HPLC was performed using a Dionex P580 isocratic pump equipped with a Varian RI detector. Antioxidant activity were measured using UV-Vis spectrophotometer (Thermo Spectronic, England) and Multi-detection microplate fluorescence spectrophotometer Synergy HT (Bio- TEK instruments, USA). All solvents used were spectral grade or were distilled from glass prior to use.

2.3 Extraction and Isolation of *Artemisia scoparia*

2.3.1 Extraction and Fractionation

The dried samples (3 kg) of *Artemisia scoparia* were chopped in small pieces, macerated, and extracted with methylene chloride (CH_2Cl_2) for 24 hour at room temperature. This step was repeated again. The extracted sample solution was concentrated to dryness *in vacuo*, yielding a sticky crude extract. The sample residue was then extracted once more with methanol (MeOH), according to the same procedure. The combined crude extracts were partitioned between methylene chloride and H_2O.

The organic layer was evaporated under reduced pressure, and the residue was repartitioned between *n*-hexane and 85% aq.MeOH. The aqueous layer was also further partitioned between *n*-BuOH and H_2O. This resulted in 4 fractions, i.e., the *n*-hexane (14.30 g), 85% aq.MeOH (28.89 g), *n*-BuOH (42.62 g), and H_2O (60.83 g) fractions (Scheme 1).

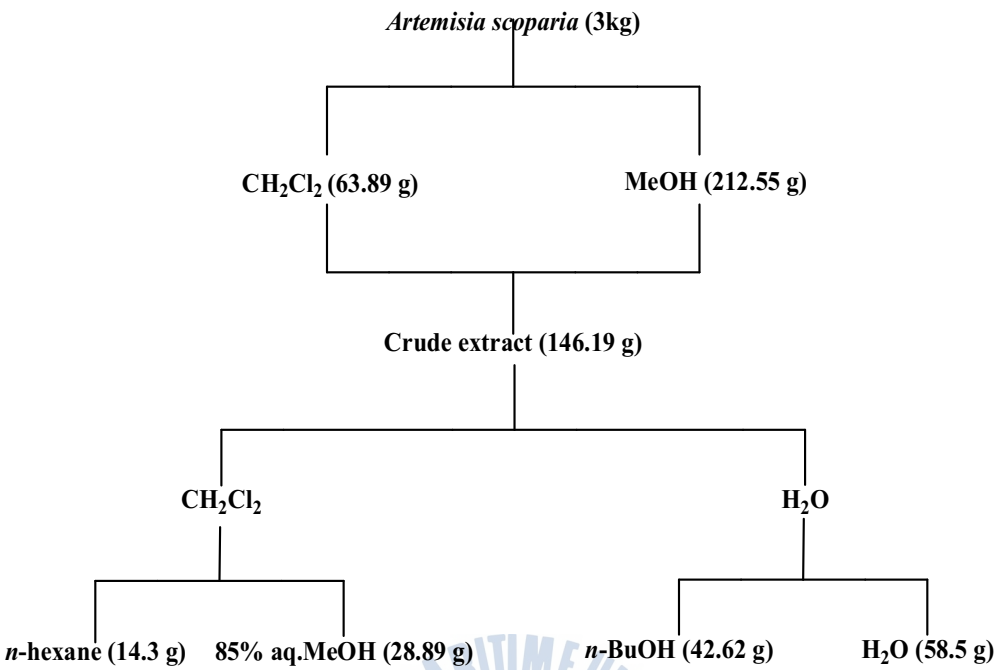

Scheme 1. Procedure of extraction and various fractions from *Artemisia scoparia*.

2.3.2 Isolation of Compounds

The *n*-hexane fraction (14.3 g) was separated into 10 subfractions by a silica column chromatography eluting with stepwise gradient mixtures of *n*-hexane/EtOAc (100% *n*-hexane, 5%, 10%, 20%, 30%, 40%, 50%, 60% and 70% EtOAc/*n*-hexane, and 100% EtOAc). The third subfraction was separated by semipreparative silica HPLC (YMC silica column, 7% EtOAc in *n*-hexane) to yield a mixture of solid (50.4 mg). Further purification of the mixture was made by reversed-phase HPLC (YMC ODS-A, 40% EtOAc in MeOH) to afford 3.7 mg of compound **2**. Further purification of the fourth subfraction by silica HPLC (YMC column, 12% EtOAc in *n*-hexane) followed by reversed-phase HPLC (YMC ODS-A, 70% aq.THF) yielded compound **1** (10.8 mg) (Scheme 2).

A portion of the *n*-BuOH fraction (10.74 g) was partitioned between EtOAc and H_2O. The EtOAc layer was evaporated on a rotary evaporator to give 3.10 g. A portion of the EtOAc (74.4 mg) was subjected to Preparative TLC on Si gel with the solvent EtOAc/MeOH/H_2O (30:5:4) to yield compound **3** (18 mg) (Scheme 3).

A portion of the 85% aq. MeOH fraction (2.0 g) was separated into seven subfractions by C18 (YMC-GEL) reversed-phase vacuum flash chromatography eluting with stepwise gradient mixtures of MeOH/H_2O (50%, 60%, 70%, 80%, and 90% aq.MeOH and 100% MeOH) and 100% EtOAc. The first fraction (2.30 g) was chromatographed on an HP-20 (DiaionTM HP-20, Supelco) with H_2O, 50% aq.MeOH, 50% aq.acetone, 100% MeOH, and 100% acetone as eluents and then the 50% aq.MeOH fraction (1.20 g) was separated by reversed-phase HPLC (YMC ODS-A, 48% aq.MeOH) followed by reversed-phase HPLC (YMC ODS-A, 40% aq. acetonitrile) to afford compound **4** (12.6 mg) (Scheme 4).

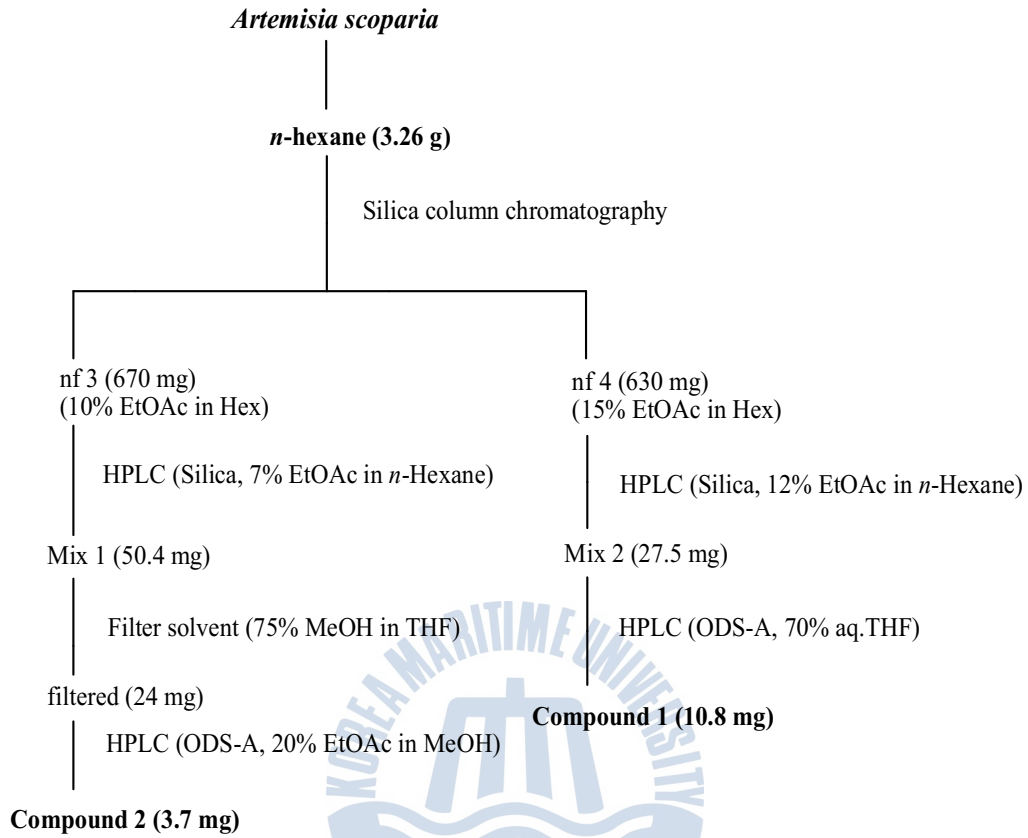

Scheme 2. Isolation procedure of compounds 1-2 from *Artemisia scoparia*.

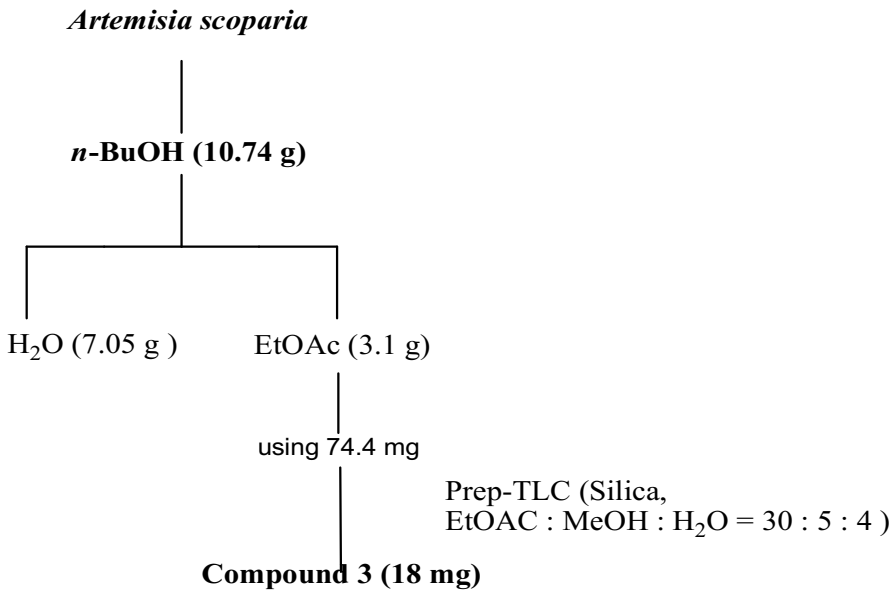

Scheme 3. Isolation procedure of compound **3** from *Artemisia scoparia*.

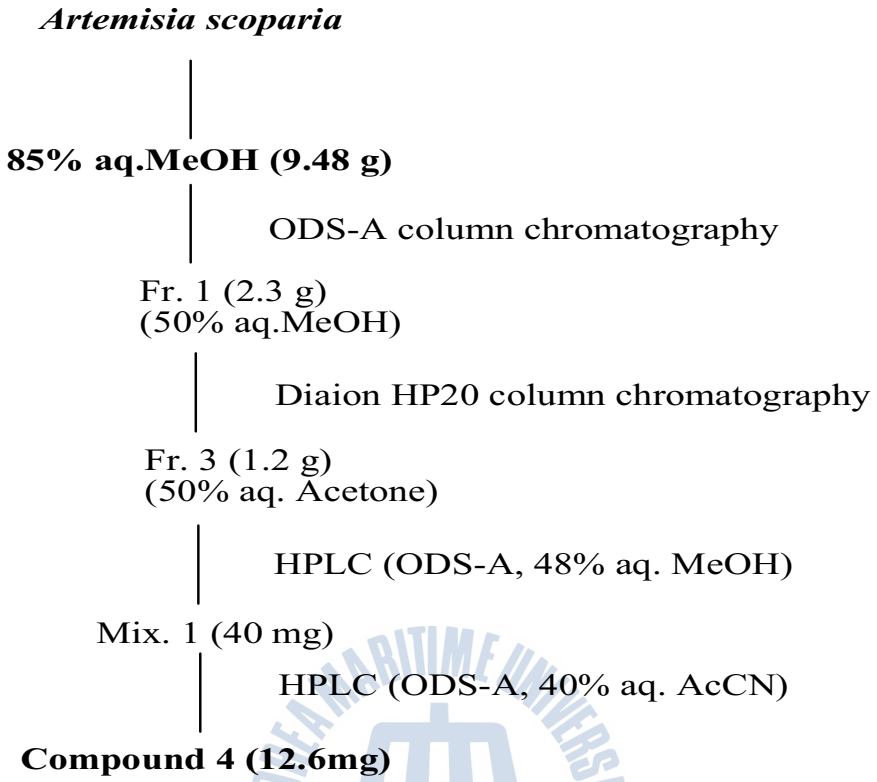

Scheme 4. Isolation procedure of compound **4** from *Artemisia scoparia*.

2.4 Antioxidant Effects

2.4.1 DPPH radical Scavenging Activity

1,1-Diphenyl-2-picryl-hydrazyl (DPPH) radical scavenging effect was evaluated according to the method employed by Blois (Blois, 1958). To 1.0 mL of DPPH methanol solution (1.5 x 10^{-1} M), 4 mL of MeOH solution of various sample concentrations was added. After mixing gently and leaving for 30 min at room temperature, the optical density was measured at 518 nm using a spectrophotometer. The scavenging activity was determined by comparing the absorbance with ashyA that of the control (100%) containing only DPPH and solvent (Figure 3) (Scheme 5).

$$EDA\,(electron\,donationg\,ability)(\%) = \frac{(control - \mathrm{exp}eriment\ )}{control\,absorbance} \times 100 \quad (1)$$

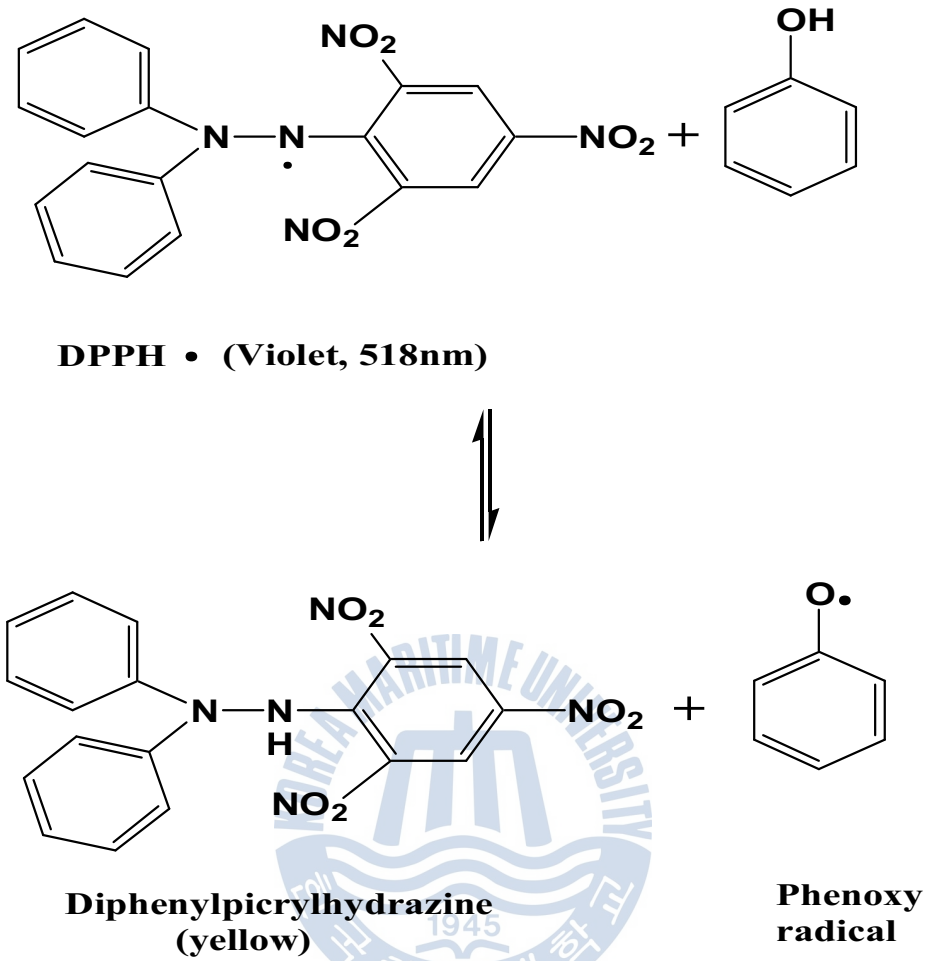

Figure 3. Scavenging of the DPPH radical by phenol.

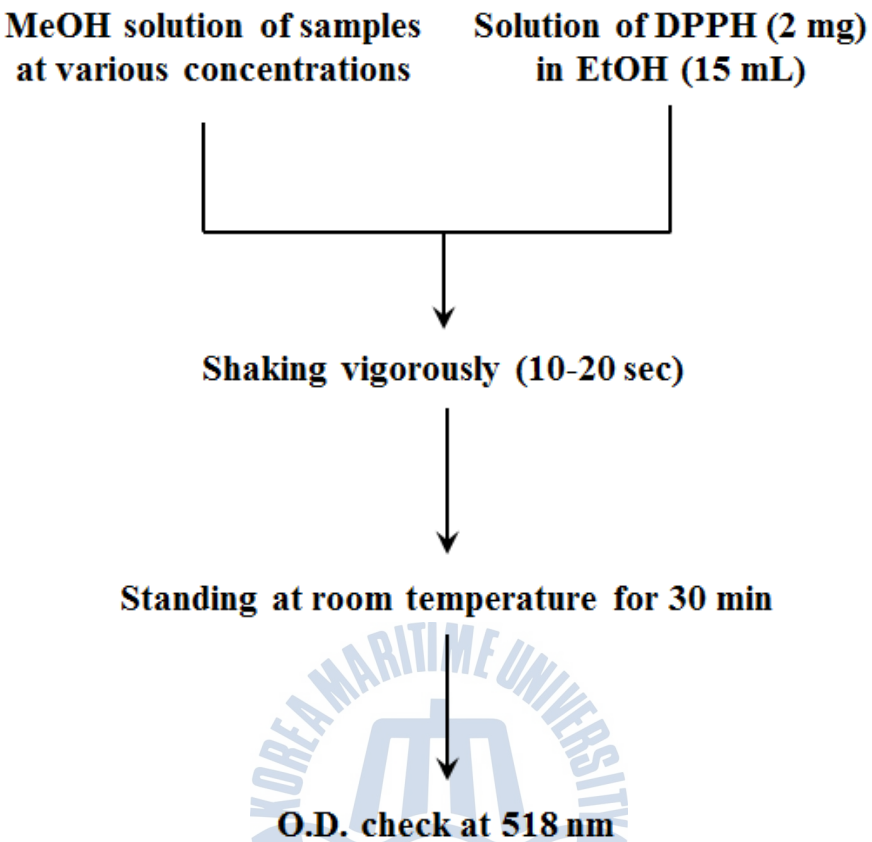

Scheme 5. Measurement of DPPH radical scavenging effect.

2.4.2 Peroxynitrite Scavenging Activity

The peroxynitrite ($ONOO^-$) scavenging ability was measured by monitoring the oxidation of dihydrorhodamine 123 using a modified version of the method (Kooy et al., 1994). The peroxynitrite reacts with DHR 123, causing oxidized DHR 123 to form, and its converted chemical structure is capable of emitting fluorescence. A stock solution of DHR 123 (5 mM) purged with nitrogen was prepared in advance and stored at -80 °C. A working solution of DHR 123 (final concentration, 5 M) was diluted from the stock solution and placed on ice in the dark immediately prior to the measurement. The buffer of 90 mM sodium chloride, 50 mM sodium phosphate (pH 7.4) and 5 mM potassium chloride with 100 M (f.c.) diethylenetriaminepentaacetic acid (DTPA) was purged with nitrogen and placed on ice before use. The $ONOO^-$ scavenging ability, based on the oxidation of DHR 123, was determined with a microplate fluorescence spectrophotometer, FL 500 (Bio-Tek instruments, USA) using the wavelengths of 485 nm and 530 nm for excitation and emission, respectively, at room temperature. The background and final fluorescent intensities were measured 5 min after treatment with or without SIN-1 (f.c. 10 M) or authentic $ONOO^-$ (f.c. 10 M) in 0.3 N sodium hydroxide. The oxidation of DHR 123 due to decomposition of the SIN-1 gradually proceeded whereas the authentic $ONOO^-$ rapidly oxidized DHR 123 with the final fluorescent intensity being stable over time. Penicillamine was used as a positive control (Figure 4) (Scheme 6).

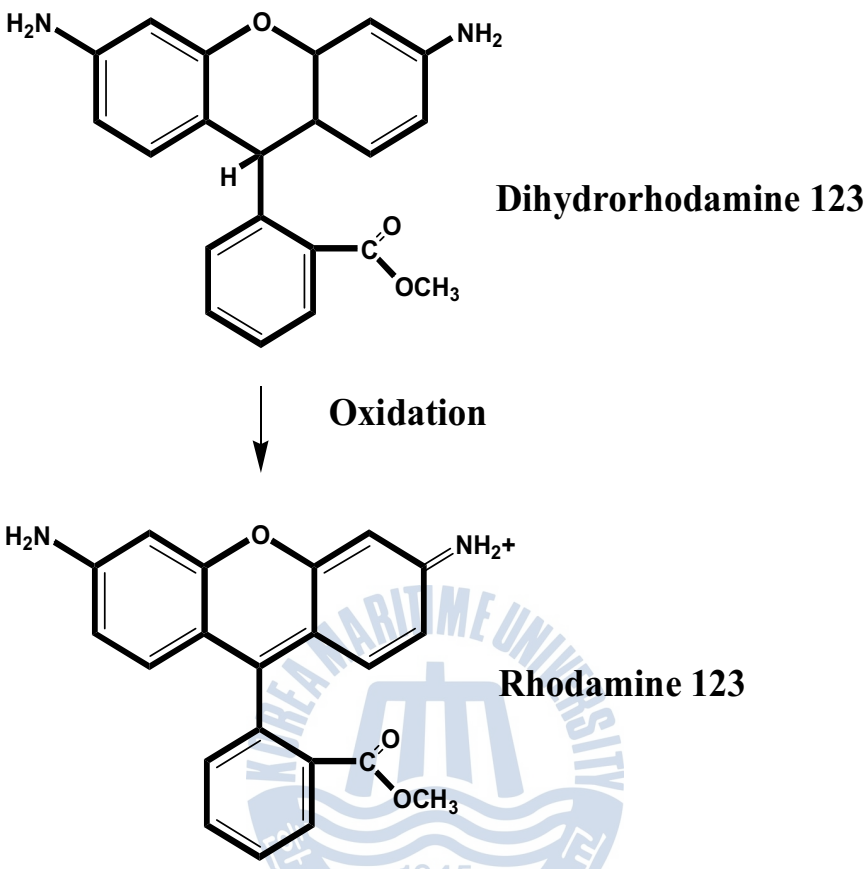

Figure 4. Peroxynitrite ($ONOO^-$) mediated oxidation of DHR123.

Diethylenetriaminepentaacetic acid (DTPA) 100 μM

↓

Dihydrorhodamine 123 5 μM

↓

Incubation at 37 ℃ for 1 min

↓

Sample

↓

SIN-1 200 μM or peroxynitrite 5 μM

↓

Measurement of fluorescence intensity
Excitation wavelength at 480 nm
Emission wavelength at 525 nm

Scheme 6. Measurement of the $ONOO^-$ scavenging effect.

2.4.3 Cell Culture

Human fibrosarcoma (HT1080) cells were grown as monolayers in T-75 tissue culture flasks (Nunc, Roskilde, Denmark) at 5% CO_2 and 37 °C humidified atmosphere using Dulbecco's modified eagle medium (DMEM, Gibco-BRL, Gaithersburg, MD, USA) supplemented with 10% foetal bovine serum (FBS), 2 mM glutamine and 100 μg/mL penicillin-treptomycin (Gibco-BRL, Gaithersburg, MD, USA). The medium was changed twice or three times a week.

2.4.4 Measurement of Cytotoxicity using MTT assay

Cytotoxic levels of the samples on cultured cells were measured using MTT assay,31) which is based on the conversion of MTT to MTT-formazan by mitochondrial enzyme. The cells were seeded onto 96-well microplates at a density of 5 x 10^3 cells/well for 24 hour. Then the cells were treated with control medium or the medium supplemented with 5 μg/mL samples. After incubation of 1 hour, 100 μl of MTT solution (1 mg/mL) was added and incubated for 4 hour. Finally, 150 μl of dimethyl sulfoxide (DMSO) was added to solubilize the formed formazan crystals, and the amount of formazan crystal was determined by measuring the absorbance at 540 nm using a multidetection microplate fluorescene spectrophotometer synergy HT (Bio-Tek Instrucments Inc., Winooski, VT, U.S.A.). Relative cell viability was determined by the amount of MTT converted into formazan crystal. Viability of cells was quantified as a percentage compared to the control, and dose response curves were developed (PR Twentyman, 1987).

2.4.5 Determination of Intracellular Formation of Reactive Oxygen Species (ROS) using DCFH-DA labelling

DCFH-DA assay used measuring free radical production in cells (Okimotoa, 2000). DCFH-DA (fluorescence probe 2,7-dichlorodihydrofluorescein diacetate, sigma) react with reactive oxygen species and than generated fluorescence. Measured fluorescence have been used to detect reactive oxygen species in Intracellular. The cells were seeded into black 96-well plates at a density of 1×10^7 cells/㎖ each well and incubated for 24 hours. After cells were washed twice in PBS, 20 μM DCFH-DA was added and incubated for 20 minutes at 37℃ in CO_2 incubator. Each well treated by varying concentrations samples and incubated 1 hours at 37℃ in CO_2 incubator. And then, remove DCFH-DA and cells were washed twice in PBS, treat 500 μM H_2O_2. Atfer than, the fluorescence intensity was measuered at excitation 360 nm and emission 465 nm after 30 minutes interval during 2 hours, using a multi-detection microplate fluorescene spectrophotometer Synergy HT (Bio-Tek instruments, USA).

2.4.6 Genomic DNA Extraction and Determination of Radical Mediated DNA damage

Genomic high molecular weight DNA was extracted from HT1080 cells using standard phenol/proteinase K procedure with slight modifications. Briefly, cells culturing in 10 cm dishes were washed twice with PBS and scraped into 1 mL of PBS containing 10 mM EDTA. After centrifugation, the cells were dissolved in RNase (0.03 mg/mL), NaOAC (0.175 M), proteinase K (0.25 mg/mL) and SDS (0.6%). The mixture was then incubated for 30 min at 37° C and 1 hour at 55° C. Following incubation, phenol:chloroform:isoamylalcohol (25:24:1) was added at 1:1 ratio and mixture was centrifuged at 6,000×g for 5 min at 4° C. Following centrifugation, supernatant was mixed with 100% ice cold ethanol at 1:1.5 ratio and kept for15 min at -20° C. After centrifugation at 16,000×g for 5 min at 4° C, the pellet was dissolved in TE buffer and purity of DNA was spectrophotometrically determined at 260/280 nm. Further, the quality of isolated DNA was evaluated with 1% agarose gel electrophoresis in 0.04 M Tris-acetate-0.001 MEDTA buffer.

H_2O_2 mediated DNA oxidation was determined by a method described elsewhere. DNA reaction mixture (100 μl) was prepared by adding various concentrations of the compounds (or same volume of distilled H_2O as control), final concentrations of 200 μ M $FeSO_4$ and 0.1 mM H_2O_2 to 50 μg/mL final concentration of genomic DNA in the same order. Then the mixture was incubated at roomtemperature for 30 min and the reaction was terminated by adding 10 mM final concentration of EDTA. Aliquot (20 μl) of reaction mixture containing about 1 μg of DNA was electrophoresed on a 1% agarose gel for 30 min at 100 V. The gels were stained with 1 mg/mL ethidium bromide and visualized by UV light using AlphaEase® gel image analysis software (Alpha Innotech, CA, USA).

2.5 Anticancer Activity Assay

2.5.1 Cell Cultures and Inhibition of Cancer Cell Proliferation

AGS (human gastric cancer), HT-29 (human colon cancer), HT1080 (human fibrosarcoma), and MCF-7 (human breast cancer) cell lines were separately grown as monolayers in T-75 tissue culture flasks in a humidified atmosphere of 95% air with 5% CO_2 at 37 ^{o}C using appropriate media supplemented with 10% fetal bovine serum (FBS), 2 mM glutamine, and 100 μg/mL penicillin-streptomycin. Dulbecco's modified eagle medium (DMEM) and RPMI 1640 were used as the culture mediums for HT1080 cells and AGS, HT-29, and MCF-7 cells, respectively. The medium was changed 2-3 times each week.

The anti-proliferative effect of the crude extract ans its fractions on cultured cells were measured using MTT [3-(4,5-dimethylthiazol-2-yl)-2,5-diphenyltetrazolium bromide] assay. The cells were grown in 96-well plates at a density of 5 x 10^3 cells/well. After 24 hour, cells were treated with different concentrations of samples. After incubation for 48 h, the cells were incubated with 100 μL of MTT (1 mg/mL) for 4 hour. Finally, the medium was removed and 100 lL of DMSO (dimethyl sulfoxide) were added to solubilize the formed formazan crystals. The amount of formazan crystal was determined by measuring the absorbance at 540 nm using a microplate spectrophotometer.

$$Cell\,viability\,(\%) = \frac{(control - \mathrm{exp}eriment\ )}{control\ absorbance} \times 100 \qquad (2)$$

2.6 Antiinflammatory Activity Assay

2.6.1 Cell Culture

Raw 264.7 macrophage cells were cultured in a 5% CO_2 and 37 ^{o}C humidified atmosphere using Dulbecco's Modified Eagle's Medium supplemented with 10% fetal bovine serum, 2 mM glutamine, and 100 mg/mL penicillin-streptomycin (all from Gibco-BRL, Gaithersburg, MD). The medium was changed two or three times each week.

2.6.2 Measurement of Cytotoxicity using MTT assay

Cytotoxic levels of the samples on cultured cells were measured using the MTT assay, which is based on the conversion of MTT to MTT-formazan by mitochondrial enzyme. The cells were grown in 96-well plates at a density of 5 x 10^3 cells per well. After 24 hour, the cells were washed with fresh medium and were treated with control medium or medium supplemented with different concentrations of the sample. After incubation for 48 h, cells were rewashed, and 100 mL of MTT solution (1 mg/mL) was added and incubated for 4 hour. Finally, 150 mL of dimethyl sulfoxide was added to solubilize the formazan crystals that formed, and the amount of formazan crystal was determined by measuring the absorbance at 540 nm using a multidetection microplate fluorescene spectrophotometer synergy (model HT, Bio-Tek Instruments). Relative cell viability was determined by the amount of MTT converted into formazan crystal. Viability of cells was quantified as a percentage compared to the control, and dose-response curves were developed.

2.6.3 Determination of Nitrite Oxide (NO) Production

Raw 264.7 cells were seeded onto 96-well plates with 2 x 10^5 cells per well using Dulbecco' Modified Eagle' Medium without phenol red and allowed to adhere overnight with pretreated test samples for 1 h. Cellular NO production was stimulated by adding 1 mg/mL (final concentration) LPS and further incubated for 48 hours. After incubation, the production of NO was determined based on the Griess reaction. In brief, 40 mL of 5 mM sulfanilamide, 10 mL of 2 M HCl, and 20 mL of 40 mM naphthylethylenediamine were added to 150 mL of culture medium. After a 15-minute incubation period at room temperature, absorbance was measured with a multidetection microplate fluorescence spectrophotometer (Synergy HT, Bio-Tek Instruments) at 550 nm. The concentrations of nitrite were calculated from regression analysis, using serial dilutions of sodium nitrite as a standard (Beda et al, 2005).

3. Results and Discussion

3.1 Isolation and Structure Determination of Compounds

The structures of three known metabolites, α-fernenol (**1**) (Table 1), α-amyrin (**2**) (Table 2), and 3,5-dicaffeoyl-*epi*-quinic acid (**3**) (Table 3) were readily determined by NMR spectral analysis and by comparison with reported data for these compounds. α-Fernenol (**1**) and α-amyrin (**2**), previously isloated from *Artemisia scoparia* was the minor metabloites, respectively while 3,5-dicaffeoyl-*epi*-quinic acid (3), known metabolite of *Artemisia scoparia* was the major metabolites (Figure 5).

Compound **4** was isolated as a colorless oil. The presence of an aromatic ring was revealed by an occurrence of several carbon signals in the region of δ 120-165 in the ^{13}C NMR spectrum and proton signals at δ 8.41 (d, J=2.4, H-2'), 8.11 (dd, J=8.8, 2.5, H-4'), and 7.03 (d, J=8.8, H-5') in the ^{1}H NMR spectrum. The carbon signals at δ 193.4 and 198.2 in the ^{13}C NMR spectrum revealed the presence of two carbonyl groups. In addition, an oxygenated quaternary carbon signal at δ 81.7 indicated the presence of hydroxy functionality.

On the basis of the above information, the chemical structure of **4** was determined by extensive 2D NMR analysis. The ^{1}H COSY and gradient HMQC experiments exhibited the presence of a 1,2,4-trisubstituted benzene moiety. The gradient HMBC data aided the assignment of the NMR signals at the benzene ring as well as the attachment of hydroxy and acetyl functionalities at the adjacent positions (^{13}C δ 131.2 and 164.8). The placement of another

carbonyl group (C-1') was also assigned by HMBC correlations between the quaternary carbons at δ 120.6 and 193.4 and adjacent protons (H-2, -2', -5', and -6'). Hydroxy group at the side chain was placed at C-3 by HMBC correlations between carbons at δ 193.4 and 81.7 and adjacent protons. Thus, the structure of **4** was determined as a 1-(3-acetyl-4-hydroxyphenyl)-3-hydroxy-3-methyl-1-butanone (Table 4).

Table 1. ^{1}H and ^{13}C NMR spectral data for compound **1** isolated from *Artemisia scoparia*.

Position	δ_H	δ_C
1	1.92(2H, dt, J=13.5, 3.3 Hz)	39.4t
2	1.62 (2H, m)	28.2t
3	3.20 (1H, dd, J=10.0, 5.8 Hz)	79.1d
4		39.3s
5	1.28 (1H, dd, J= 10.5, 3.5 Hz)	44.3d
6	1.63 (2H, m)	19.3t
7	1.64 (2H, m), 1.35 (2H, m)	18.1t
8	2.0 (1H, dd, J=13.8, 2.5Hz)	40.1d
9		150.9s
10		37.7s
11	5.27 (1H, m, J=2.5 Hz)	116.1s
12	1.51 (2H, m)	36.8t
13		37.9s
14		36.7s
15	1.22 (2H, m)	29.4t
16	1.41 (2H, m)	36.2t
17		43.0s
18	1.52 (1H, m)	52.0d
19	1.33 (1H, m), 1.23 (1H, m)	20.2t
20	1.19 (2H, m)	28.3t
21	0.98 (1H, m)	59.7d
22	1.26 (1H, m)	30.9d
23	0.96 (3H)	27.5q
24	0.86 (3H)	15.2q
25	1.06 (3H)	25.3q
26	0.72 (3H)	15.5q
27	0.80 (3H)	16.0q
28	0.75 (3H)	14.1q
29	0.88 (3H, d, J=6.6 Hz)	22.2q
30	0.82 (3H, d, J=6.6 Hz)	23.1q

Measured in $CDCl_3$ at 300 and 75 MHz, respectively. Assignments were aided by ^{1}H COSY, TOCSY, DEPT, gHMQC and gHMBC experiments.

Table 2. ^{1}H and ^{13}C NMR spectral data for compound **2** isolated from *Artemisia scoparia*.

Position	δ_H	δ_C
1	1.68 (2H, t, J=3.5 Hz)	38.8t
2	1.60 (2H, m)	27.4t
3	3.21 (1H, dd, J=11.2, 5.1 Hz)	79.0d
4		38.8s
5	0.74 (1H, dd, J=10.1, 1.4 Hz)	55.2d
6	1.54 (1H, m), 1.40 (1H, m)	18.5t
7	1.54 (1H, m), 1.37 (1H, m)	33.0t
8		40.1s
9	1.51 (1H, m)	47.8d
10		37.0s
11	1.90 (2H, m)	23.5t
12	5.11 (2H, dd, J=3.6 Hz)	124.3d
13		139.5s
14		42.0s
15	1.83 (2H, td, J=13.4, 4.6 Hz)	26.7t
16	2.00 (2H, td, J=13.4, 4.7 Hz)	28.1t
17		33.8s
18	1.32 (1H, d, J=4.4 Hz)	59.1d
19	1.32 (1H, m)	39.7d
20	0.92 (1H, m)	39.6d
21	1.42 (2H, m)	31.3t
22	1.88 (dt, J=7.0, 3.0 Hz)	41.6t
23	0.99 (3H, s)	28.2q
24	0.79 (3H, s)	15.7q
25	0.79 (3H, s)	15.8q
26	0.95 (3H, s)	17.0q
27	1.06 (3H, s)	23.4q
28	1.00 (3H, s)	28.8q
29	0.90 (3H, d, J=6.0 Hz)	17.6q
30	0.77 (3H, d, J=7.0 Hz)	21.5q

Measured in $CDCl_3$ at 300 and 75 MHz, respectively. Assignments were aided by ^{1}H COSY, TOCSY, DEPT, gHMQC and gHMBC experiments.

Table 3. ^{1}H and ^{13}C NMR spectral data for compound **3** isolated from *Artemisia scoparia*.

Position	δ_H	δ_C
1		76.3s
2	2.11 (2H, m)	40.6t
3	5.55 (1H, dt, J=10.0, 5.8 Hz)	72.4d
4	3.91 (1H, dd, J=9.9, 3.4 Hz)	73.0d
5	5.39 (1H, m)	74.4d
6	2.04 (1H, m), 2.28 (1H, dd, J=15.2, 3.4 Hz)	37.5t
1 '		127.8s, 128.0s
2 '	7.06, 7.08 (each 1H, d, J=2.0 Hz)	115.2d
3 '		146.8s, 146.9s
4 '		149.2s, 149.4s
5 '	6.78 (2H, d, J=8.2 Hz)	116.4d
6 '	6.96, 6.97 (each 1H, dd, J=8.2, 2.0 Hz)	122.9d
7 '	7.59, 7.62 (each 1H, d, J=15.8 Hz)	146.6d, 146.6d
8 '	6.31, 6.43 (each 1H, d, J=15.8 Hz)	115.4d, 115.9d
9 '		169.0s, 169.4s
COOH		181.3s

Measured in $CDCl_3$ at 300 and 75 MHz, respectively. Assignments were aided by ^{1}H COSY, TOCSY, DEPT, gHMQC and gHMBC experiments.

Table 4. ^{1}H and ^{13}C NMR spectral data for compound **4** isolated from *Artemisia scoparia*.

Position	δ_H	δ_C
1		193.4s
2	2.83 (2H, s)	48.2t
3		81.7s
4	1.48 (3H, s)	26.8q
5	1.48 (3H, s)	26.8q
1 '		120.6s
2 '	8.41 (1H, d, J=2.5 Hz)	128.7d
3 '		131.2s
4 '		164.8s
5 '	8.11 (1H, dd, J=8.8, 2.5 Hz)	136.6d
6 '	7.03 (1H, d, J=8.8 Hz)	120.0d
1 "		198.2s
2 "	2.58 (3H, s)	26.5q

Measured in $CDCl_3$ at 300 and 75 MHz, respectively. Assignments were aided by ^{1}H COSY, TOCSY, DEPT, gHMQC and gHMBC experiments.

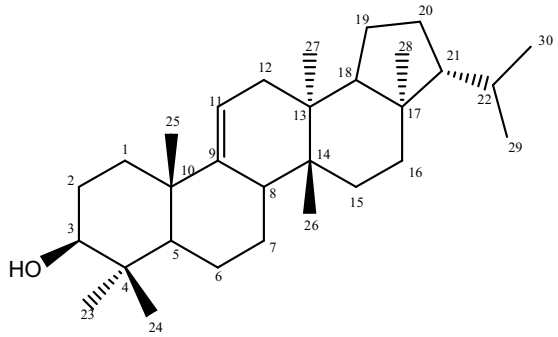

Compound **1**

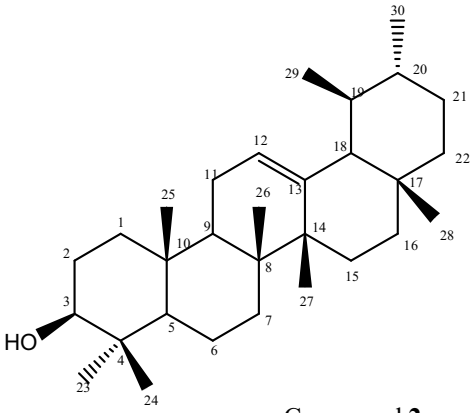

Compound **2**

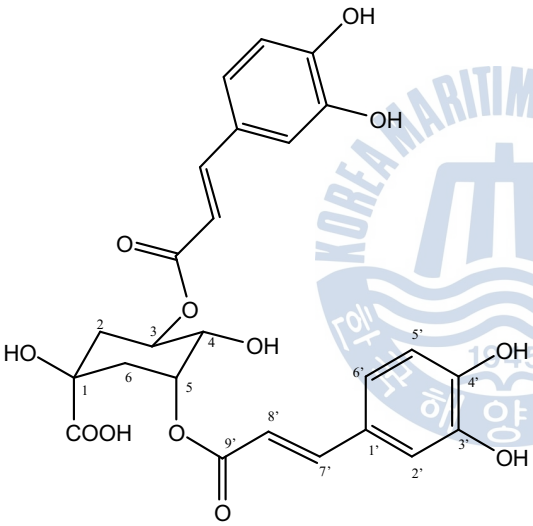

Compound **3**

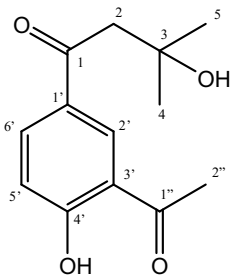

Compound **4**

Figure 5. Chemical structure of compounds **1-4** from *Artemisia scoparia*

3.2 Antioxidant Effects

3.2.1 DPPH radical Scavenging Activity

DPPH radical scavenging effect was measured at the concentrations of 1, 10, 50, 100 and 200 μg/mL of the samples the crude extract, *n*-hexane, 85% aq.MeOH, *n*-BuOH and H_2O fractions. The results exhibited that the scavenging effect increased in a dose-dependently. Crude extract, *n*-hexane, 85% aq.MeOH, *n*-BuOH and H_2O fractions show the scavenging activity of 30.3, 15.9, 31.3, 86.2 and 26.9% at the concentration of 200 μg/mL. Of them, *n*-BuOH fraction showed the highest scavenging activity 94.3%, compared with vitamin C, the control group, at the concentration of 200 μg/mL (Figure 6).

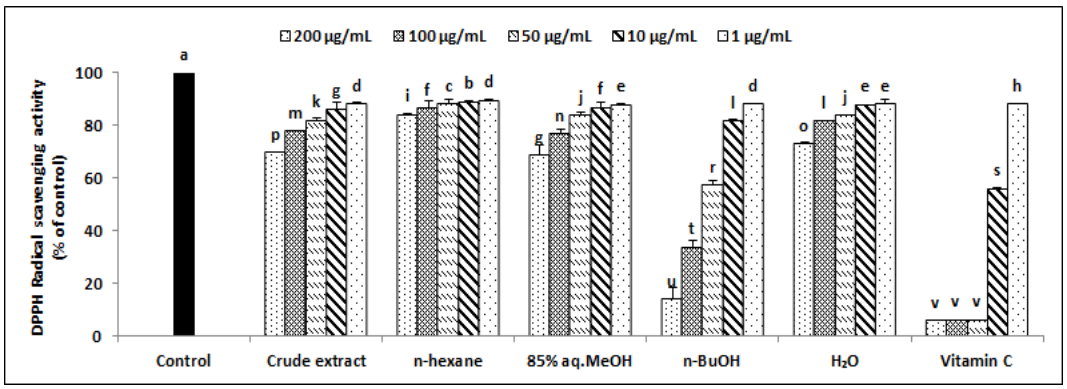

Figure 6. DPPH radical scavenging effect of crude extracts and its solvent fractions from *Artemisia scoparia*.

[a-f]Means with the different letters are significantly different ($p<0.05$) by Duncan's multiple range test.

3.2.2 Peroxynitrite Scavenging Activity

The scavenging effect of the crude extract and its solvent fractions on the authentic peroxynitrite is shown in Figure 7, where vitamin C and penicillamine (PA) were used as the positive control groups. Crude extract, 85% aq.MeOH, *n*-BuOH and H_2O fractions showed high scavenging rate more than 90% at a concentration of 200 μg/mL, showing 83.7%, 90.1%, 98.3% and 87.4% even at a concentration of 50 μg/mL in their scavenging ratio, respectively. *n*-BuOH fraction exhibited the highest scavenging rate, comparable to that of the control group (vitamin C).

The scavenging activity of peroxynitrite induced from the decomposition of SIN-1 was also evaluated. As a result, crude extract, *n*-hexane, 85% aq.MeOH, *n*-BuOH and H_2O fractions showed the scavenging rate of 72.7%, 29.8%, 91.6%, 39.5%, and 52.1% respectively at a concentration of 200 μg/mL. Of them, 85% aq.MeOH fraction showed the strongest scavenging effect, similar to that of the control group (penicillamine) (Figure 8).

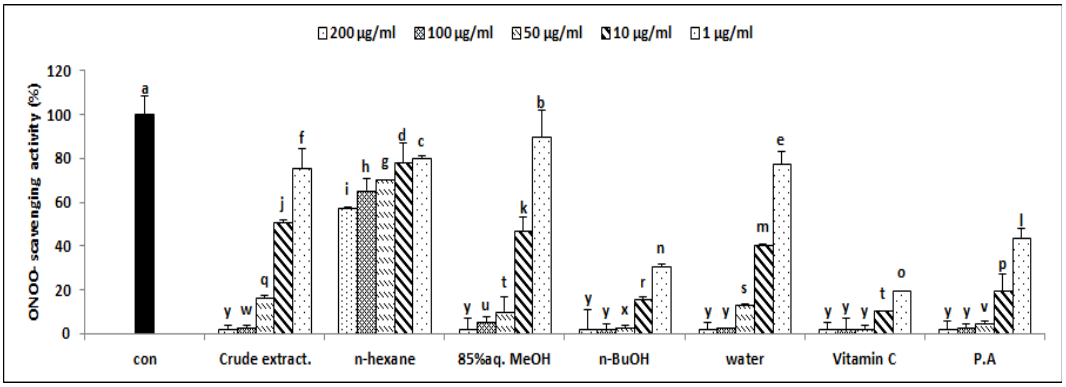

Figure 7. Scavenging effects of crude extract and its solvent fractions from *Artemisia scoparia* on authentic $ONOO^-$.

[a-f]Means with the different letters are significantly different ($p<0.05$) by Duncan's multiple range test.

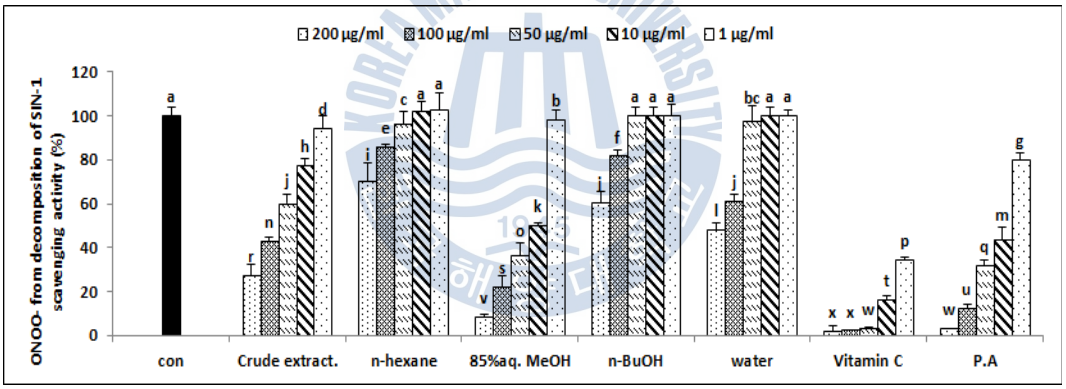

Figure 8. Scavenging effects of crude extract and its solvent fractions from *Artemisia scoparia* on $ONOO^-$ from SIN-1.

[a-f]Means with the different letters are significantly different ($p<0.05$) by Duncan's multiple range test.

3.2.3 Determination of Intracellular Formation of ROS using DCF-DA Labeling

The antioxidant effect of all the samples was investigated on human fibrosarcoma HT1080 cells. In order to avoid cytotoxic interference of these compounds at high concentrations, the influence of the sample on cell viability of HT1080 cells was determined using MTT assay. No significant toxic effect was observed on the cells treated with these extracts and solvent fractions up to the concentration of 100 μg/mL during 1 hour incubation (Figure 9). The cell viabilities of HT1080 cells were 83, 89, 96, 95 and 95%, respectively, at the concentration of 200, 100, 50, 10 and 1 μg/mL for crude extract; 77, 88, 96, 98 and 97% for *n*-hexane; 75, 90, 97, 99 and 98% for 85% aq.MeOH; more than 85% for *n*-BuOH and H_2O.

The reactive oxygen species existing within cells were measured using 2', 7'-Dichlorodihydrofluorescein diacetate (DCFH-DA). DCF-DA crosses cell membranes and is hydrolyzed enzymatically by intracellular esterase to nonfluorescent DCFH. Generation of intracellular ROS such as H_2O_2 and hydroxyl radical oxidizes DCFH to highly fluorescent DCF in cells. The degree of fluorescence was measured at intervals of 30 minutes for 120 minutes. The radical scavenging effects were compared to the control treated only with H_2O_2, and the blank treated with both samples and H_2O_2, respectively. In the control, DCF flourescence value continued to increase whereas in the blank, DCF flourescence value remained almost unchanged with time. As shown in Figure 10, the scavenging effect of crude extract and its solvent fractions on ROS increased in a dose-dependant manner when compared to both the control group and the blank. The scavenging ratios of crude extract, *n*-hexane, 85% aq.MeOH and *n*-BuOH fractions on intracellular ROS were 41.3, 38.4, 52.6, and 38%, respectively, at 200 μg/mL; 19.3%, 29.6%, 41.4% and 32.9% at 100 μg/mL.

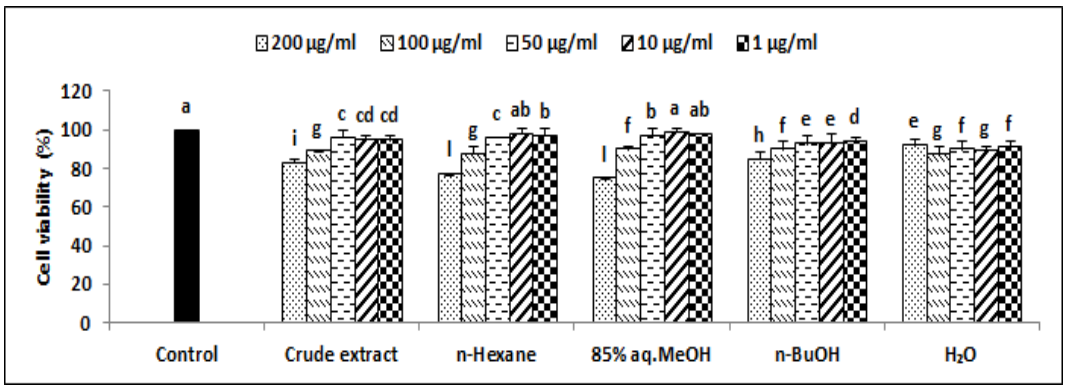

Figure 9. Effect of crude extract and its solvent fractions from *Artemisia scoparia* on viability of HT1080 cells.

[a-f]Means with the different letters are significantly different ($p<0.05$) by Duncan's multiple range test.

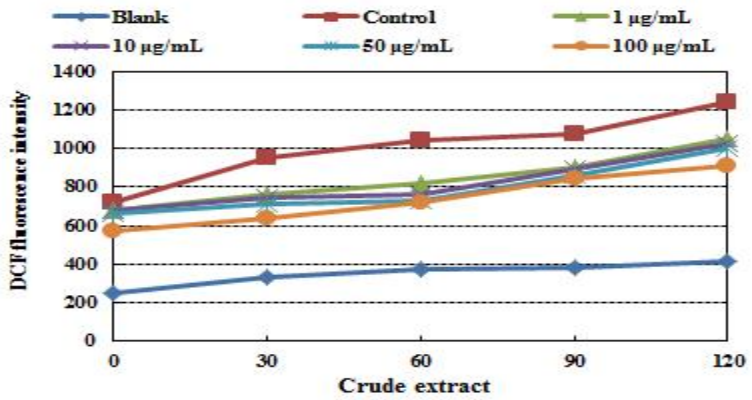

(a)

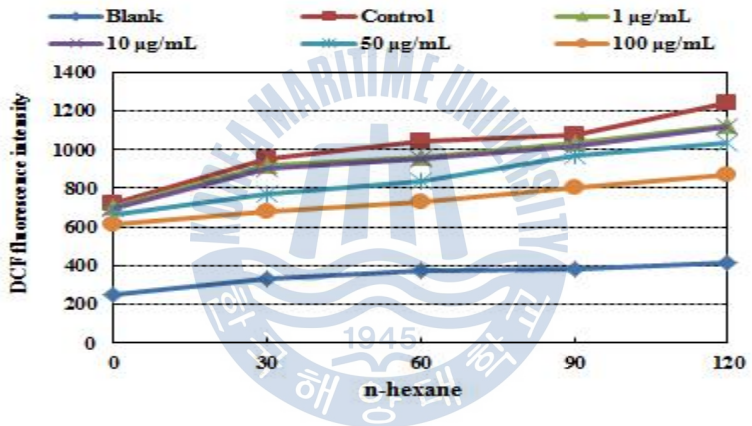

(b)

Figure 10. Scavenging effects of crude extract and its solvent fractions from *Artemisia scoparia* on intracellular ROS levels induced by hydrogen peroxide in HT1080 cells. The cells were incubated with different concentrations (100, 50, 10, 1 μM) of the samples for the indicated times respectively. DCF fluorescence was measured at $\lambda_{excitation}$ = 485 nm and $\lambda_{emission}$ = 528 nm.: (a) crude extract; (b) *n*-hexane; (c) 85% aq.MeOH; (d) *n*-BuOH; (e) H_2O.

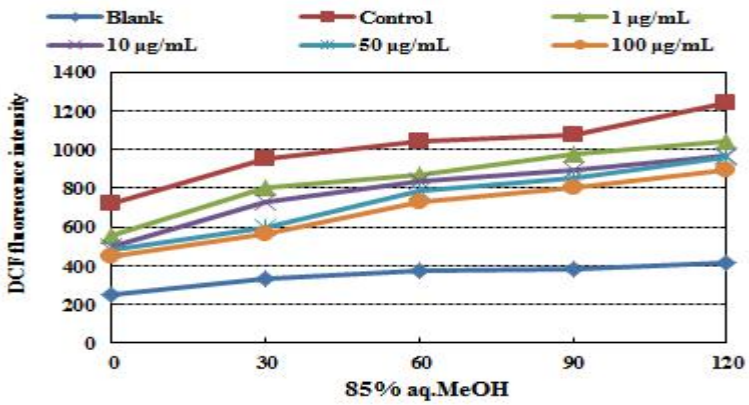

(c)

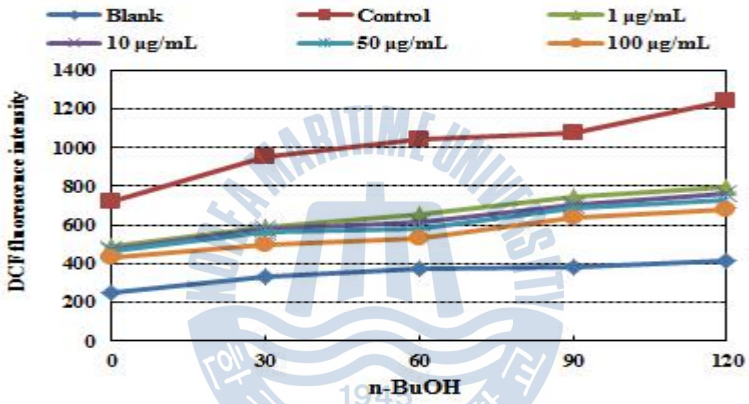

(d)

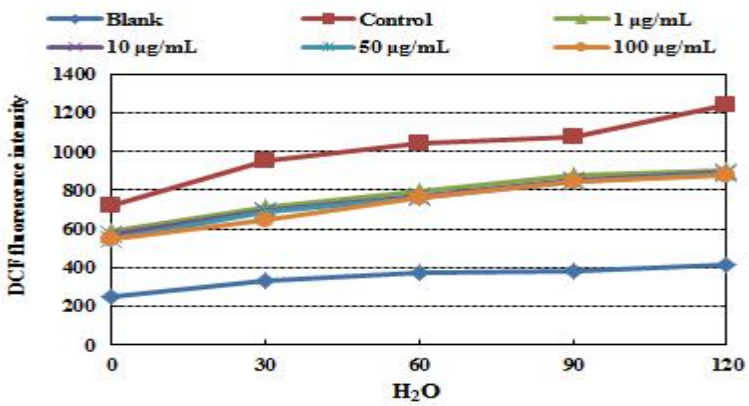

(e)

Figure 10. (continued)

3.2.4 Genomic DNA Extraction and Measurement Genomic DNA Oxidation

The effect of the crude extract of *Artemisia scoparia* on DNA oxidation was measured at the concentration of 200, 100 and 50 μg/mL. The results showed *n*-hexane and 85% aq.MeOH fractions dose-dependently inhibited the radical-mediated DNA damage, indicating a significant effect when compared to the control group (Figure 11).

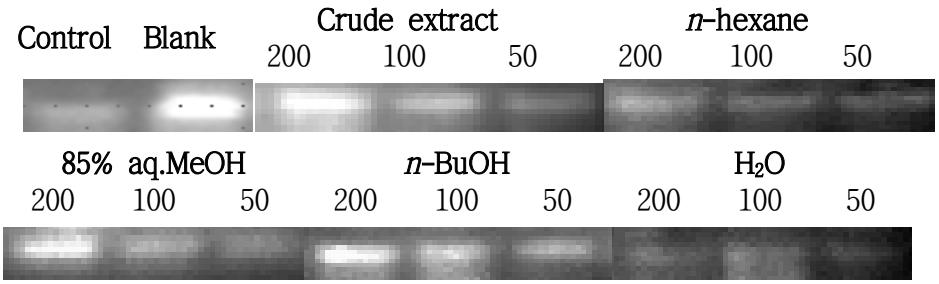

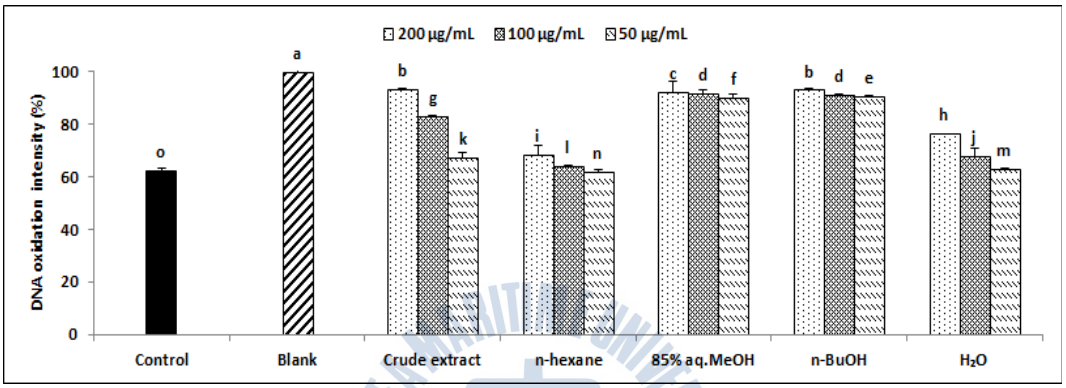

Figure 11. Antioxidant effects of crude extract and its solvent fractions from *Artemisia scoparia* on genomic DNA oxidation from HT1080 cells.

[a-f]Means with the different letters are significantly different ($p<0.05$) by Duncan's multiple range test.

3.3 Antiproliferative Effects of Crude Extract and Its Fractions from *Artemisia scoparia* in Cancer Cells

3.3.1 Effects of Crude Extract and Its Fractions on Cancer Cell Growth

The *in vitro* cytotoxic activity of the extracts and fractions was assessed using four different human tumour cell lines: stomach (AGS), colon (HT-29), fibrosarcoma (HT1080), and breast (MCF-7). The extracts and solvent fractions were used at concentrations ranging from 1 to 200 μg/mL.

n-Hexane and 85% aq.MeOH fractions exhibited the potent antiproliferative effects on human cancer cell lines in a dose-dependent manner ($p < 0.05$). In the comparative analysis, *n*-hexane fraction exhibited the inhibitory rates of more than 77% against all human cancer cells except MCF-7 at a concentration of 200 μg/mL. 85% aq.MeOH fraction inhibited proliferation of all human cancer cells in a ratio of more than 80%.

In case of 100 μg/mL dose, 85% aq.MeOH fraction of all tested samples exerted the strongest antiproliferative effect against HT1080, AGS, HT-29 and MCF-7 cells with inhibitory rates of 59.7, 98.3, 87.9 and 46.4%, respectively (Figure 12). *n*-Hexane fraction showed the good antiproliferative effect against HT1080 (74.4%) and AGS (72.1%).

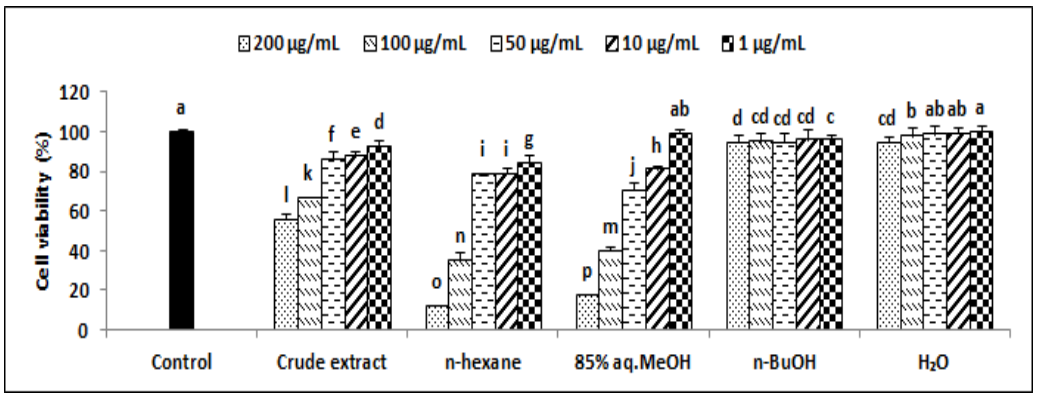

(a)

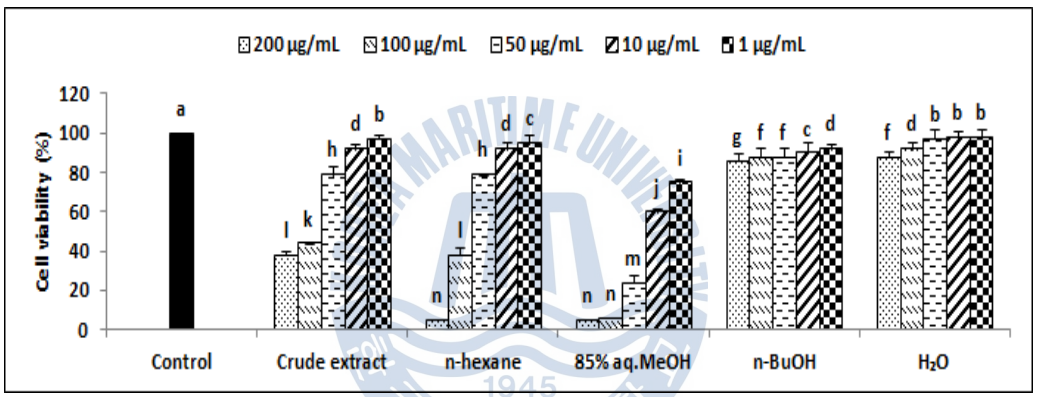

(b)

Figure 12. Antiproliferative effect of crude extract and its solvent fractions from *Artemisia scoparia* on viability of cancer cells.

[a-f]Means with the different letters are significantly different ($p<0.05$) by Duncan's multiple range test : (a) HT1080; (b) AGS; (c) HT-29; (d) MCF-7.

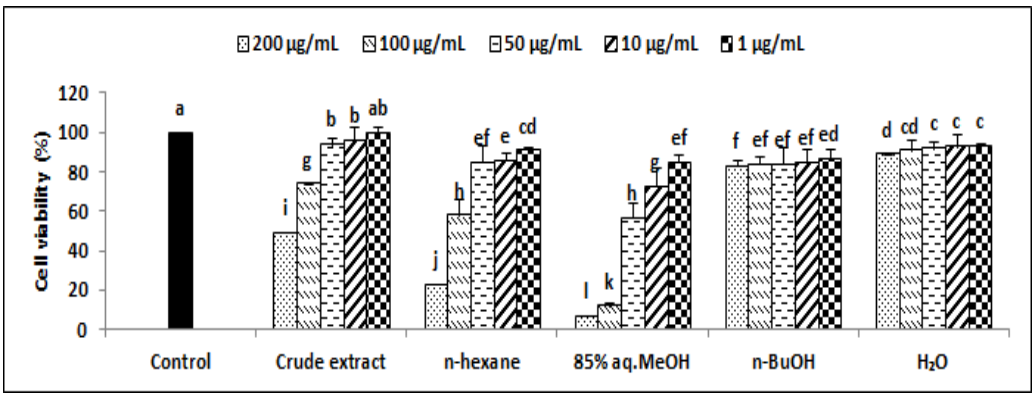

(c)

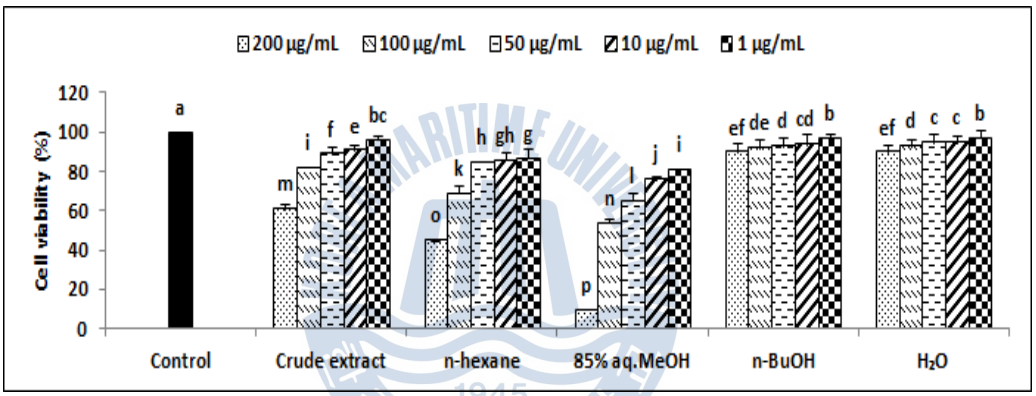

(d)

Figure 12. (continued)

3.4 Inhibitory Effect of Nitric Oxide (NO) Production

In order to evaluate whether the *Artemisia scoparia* exhibits antiinflammatory effect, the inhibitory effect of crude extract and its solvent fractions on NO production was examined using an *in vitro* model system of Raw 264.7 cells stimulated with LPS (lipopolysaccharide). All samples were diluted to 100, 50, 10 and 1 μg/mL each before being used for this bioassay test. The control treated only with LPS and the blank not treated with both samples and LPS were used for the comparative analysis. The results showed the crude extract significantly inhibited production of NO in a ratio of 43.8, 35.7, 16.8 and 10.1%, respectively, at the concentrations of 100, 50, 10 and 1 μg/mL. *n*-Hexane and 85% aq. MeOH fractions also revealed the significant inhibition of NO production in LPS-activated macrophases (Figure 13).

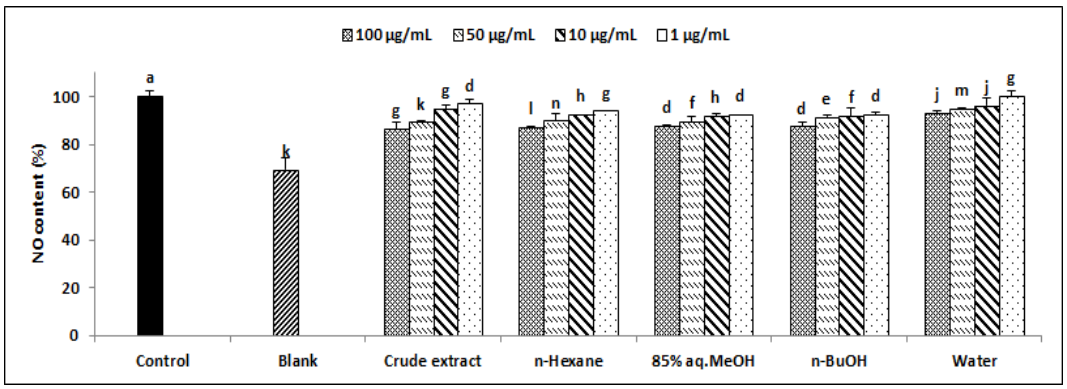

Figure 13. Effects of crude extract and solvent fractions from *Artemisia scoparia* on nitrite production in Raw 264.7 cells (100, 50, 10, 1 μg/mL).
[a-f]Means with the different letters are significantly different ($p<0.05$) by Duncan's multiple range test.

4. Conclusion

Most organisms living on the earth have various organic materials, produced via the metabolic pathway in the body. The development of new biofuntional materials such as new medicines and dietary supplements from these natural substances is a key part of study in medicinal chemistry and biotechnology. The industrial importance of natural products is shown by the fact that over 1/3rd of the drugs currently used were obtained from natural products or their synthetic derivatives. Because of the great increase in multi-drug resistance, many efforts have focused on developing new drugs working through unique mechanistic pathway. Therefore, natural products have received considerable attention as promising sources for the development of these new types of drugs. The global pharmaceutical industries are actively obtaining exclusive patents and continuing to develop another new biological resources.

As part of our search for bioactive substances from marine resources, the halophyte *Artemisia scoparia* Wald. et Kitaib was collected from tidal flats along the western coast of Korea. Two different crude extracts were obtained through the extraction of *Artemisia scoparia* Wald. et Kitaib (directly collected from the Ganghwa Island) with methylene chloride and methanol. These extracts were combined to obtain four solvent fraction fractions based on polarity of *n*-hexane, 85% aq.MeOH, *n*-BuOH, and H_2O. The antioxidant capacity of each fraction was investigated; this analysis indicated that the *n*-BuOH fraction exhibited the greatest antioxidant effects, with a DPPH radical scavenging rate of 86% at a concentration of 200 μg/mL. The 85%

aq.MeOH and *n*-BuOH fractions showed the highest suppression ratio on generation of the intracellular ROS in HT1080 cells and oxidation of DNA isolated from HT1080 cells, respectively. The 85% aq.MeOH fraction also exhibited the highest scavenging effect on peroxynitrite induced from SIN-1, displaying 91% in a scavenging ratio at a concentration of 200 μg/mL.

In cytotoxicity assay, 85% aq.MeOH fraction exhibited the good inhibition effect against four types of human cancer cells: 59.7% for HT1080; 98.3% for AGS; 87.9% for HT-29; 46.4% for MCF-7 at a concentration of 100 μg/mL, respectively. The *n*-hexane fraction also showed the significant growth inhibitory effects on all cancer cells except MCF-7 at a concentration of 100 μg/mL.

A total of four compounds were obtained by bioassay-guided separation, and their chemical structures were determined by 2D NMR experiments and by comparison with published spectral data. α-Fernenol **(1)** and α-amyrin **(2)**, two known triterpenoids (Szakiel A1, 2012) were separated from the *n*-hexane fraction. 3,5-Dicaffeoyl-*epi*-quinic acid **(3)**, previously reported from *Chrysanthemum morifolium* (Kim, Hyoung Ja, 2005) was also separated from the *n*-BuOH layer. 1-(3-Acetyl-4- hydroxyphenyl)-3-hydroxy-3-methyl-1-butanone **(4)**, a new compound, was separated from the 85% aq.MeOH fraction.

Recently, antibacterial activity of α-fernenol against *Colletotrichum gloeosporioides* (Punnawich Yenjit, 2010) was reported. α-Amyrin has interesting biological activities, such as modulation of hepatic oxidative stress (Dharmendra Singh, 2015), relief from constant neuropathic pain (Kathryn A.B. Simão da Silva, 2011), reduction of the rate of apoptosis of HL-60 leukemia cells (Francisco W.A. Barros, 2011), and enhancement of the erectile functions of mice (Pierre Watcho, 2012). 3,5-Dicaffeoyl-*epi*-quinic acid is known to activate antioxidation and suppress AKR1B10 (Lee, Joo-Young, 2009), a target for cancer treatment. The biological activity of the novel compound, 1-(3-acetyl-4-hydroxyphenyl)-3-hydroxy-3-methyl-1-butanone **(4)**, is under investigation.

Acknowledgement

어느새 2년의 대학원 생활이 흘러갔습니다. 석사생활을 돌이켜보니 처음 실험실에 들어올 때 가졌던 각오, 설렘 그리고 두려움이 생각납니다. 처음 제가 실험을 배우던 시간들이 마치 어제 일처럼 생생합니다. 석사 2년 동안 아쉬웠던 점도 많고 성취감을 느꼈던 점도 많았습니다. 너무나 부족했지만 학위 논문을 끝내고 이렇게 감사의 글을 쓸 수 있다는 것만으로도 가슴이 벅차오릅니다.

먼저 정신적, 학문적인 냉철함으로 지도해 주시고 석사 학위 논문을 무사히 마칠 수 있도록 바쁘신 와중에도 성심성의껏 지도해주신 서영완 지도교수님께 진심으로 감사드립니다. 그리고 학문적 조언과 격려를 아낌없이 해주신 해양과학기술전문대학원 교수님들, 저를 믿고 지원해준 해양과학기술전문대학원에 큰 감사를 드립니다. 또 석사 처음 시작할 때 실험에 관해 아무것도 모르던 나에게 바쁜 시간을 쪼개서 이끌어주고 도와준 명국이, 생전 처음 해보는 세포실험을 알려주고 도와준 호준이, 그리고 실험실 정리를 잘 해준 승오, 실험실 처음 들어와서 배울 것도 많고 바쁠 시기에도 나를 많이 도와줬던 은신이, 희정이 그리고 내가 처음 실험실에 들어올 때와 비슷해서 걱정이 많았지만 잘 적응해준 혜림이, 다른 대학원생인데도 불구하고 저에게 조언과 도움을 아끼지 않았던 형주언니, 힘들 때 옆에서 많이 도와준 선미와 유진이에게 감사드립니다.

그리고 무엇보다 언제나 든든한 버팀목이 되어주고 제가 이 자리에 있도록 도와주신 어머니 아버지께 감사의 말씀드리고 싶고 이 논문을 바칩니다. 이제는 이러한 가족들의 은혜에 조금이나마 보답할 수 있도록 노력하겠습니다.

마지막으로 그 동안 저를 도와주시고 이끌어주신 분들께 다시 한번 감사드립니다.

References

김웅서, 2012, *해양과학기술의 현재와 미래*, 한국해양과학기술원

이우철, 1996, *원색한국기준식물도감*, 아카데미서적.

Arató E. et al., 2006, Oxidative stress and Leukocyte activation after lower limp revasclarization surgery. *Magy. Seb.*, 59, pp.50-57.

Blois M. S., 1958, Antioxidant determinations by the use of a stable free radical, *Nature*, 25, pp.1199-1200.

Beda, N., and A. Nedospasov, 2005, A spectrophotometric assay for nitrate in an excess of nitrite. *Nitric Oxide*, 13, pp.93-97.

Choi, E. Park, H. Lee & J. Kim, 2013, Anticancer, antiobesity, and anti-inflammatory activity of Artemisia species in vitro, *Journal of traditional Chinese medicine*, 33(1), pp.92-97.

Chen, Y. et al., 2005, Involvement of protein kinase C in the inhibition of lipopolysaccharide-induced nitric oxide production by Thapsigargin in RAW 264.7 Macrophages, *Int. J. Biochem.* Cell B., 37, pp.2574-2585.

Dharmendra Singh et al., 2015, Modulatory potential of α-amyrin against hepatic oxidative stress through antioxidant status in wistar albino rats, *Journal of Ethnopharmacology*, 161(23), pp.186-193.

Francisco W.A. Barros et al., 2011, Amyrin esters induce cell death by apoptosis in HL-60 leukemia cells, *Bioorganic & Medicinal Chemistry*, 19(3), pp.1268-1276.

Green L. C., et al., (1982), Analysis of Nitrate, Nitrite, and [15N] Nitrate in Biological Fluids. *Anal. Biochem.*, 126, pp.131-138.

Habib M., Waheed I., 2013, Evaluation of anti-nociceptive, anti-inflammatory and antipyretic activities of *Artemisia scoparia* hydromethanolic extract, *Journal of ethnopharmacology* , 145(1), pp.18-24.

Hyoung Ja Kim & Yong Sup Lee, 2005, Identification of new dicaffeoylquinic acids from *Chrysanthemum morifolium* and their antioxidant activities, Planta medica, 71(9), pp.871-876.

Jung-Ah Seo, et al., 2009, ANTIMICROBIAL ACTIVITY OF ARTEMISIA SPECIES AGAINST CLINICALLY ISOLATED STREPTOCOCCUS MUTANS, *Journal of the Korean academy of pediatric dentistry,* 36(4), pp.505-513.

Kim C. H., Lee K. B., Cho D. S. & Myoung H, 2006, The Study on the Flora and Vegetation of Salt Marshes of Mankyeong River Estuary in Jeonbuk, *Korean Journal of Pharmacognosy*, 20(3), pp.289-298.

Kathryn A.B. Simão da Silva et al., 2011, Activation of cannabinoid receptors by the pentacyclic triterpene α, β-amyrin inhibits inflammatory and neuropathic persistent pain in mice, *PAIN®*, 152(8), pp.1872-1887.

Kooy, N. W., J. A. Royall, H. Ischiropoulos & J. S. Beckman, 1994, Peroxynitrite-mediated oxidation of dihydrorhodamine 123, *Free Radical Biology & Medicine*, 16, pp.149-156.

Lee, H. J. and Seo, Y., 2006, Antioxidant properties of Erigeron annuus extract and its three phenolic constituents, *Biotechnol. Bioprocess Eng.*, 11, pp.13-18.

Lee, H. J. et al., 2004, Screening of peroxynitrite and DPPH radical scavenging activities from salt marsh plants. *Korea J. Biotechnol. Bioeng.*, 19, pp.57-61.

Lee, Joo-Young et al., 2009, Inhibitory Effects of 3,5-O-Dicaffeoyl-epi-quinic Acid from Gymnaster koraiensis on AKR1B10, *Journal of applied biological chemistry*, 52(6), pp.731-734.

Muhammad Shaiq Ali & Muhammad Jahangir, 2008, Scoparal: A New Aromatic Constituent from *Artemisia Scoparia* Waldst, *The Journal of the Chemical Society of Pakistan*, 30(4), pp.609-611.

Okimotoa, Y. et al., 2000, A novel fluorescent probe diphenyl-1-pyrenylphosphine to follow lipid peroxidation in cell membranes. *FEBS Lett*, 474, pp.137-140.

PR Twentyman & M Luscombe, 1987, A study of some variables in a tetrazolium dye (MTT) based assay for cell growth and chemosensitivity, British journal of cancer, 56(3), pp.279-285.

Punnawich Yenjit, Montree Issarakraisila, Warin Intana & Kan Chantrapromma, 2010, Fungicidal activity of compounds extracted from the pericarp of Areca catechu against Colletotrichum gloeosporioides in vitro and in mango fruit, *Postharvest Biology and Technology*, 55(2), pp.129-132.

Pierre Watcho et al., 2012, Enhancement of erectile function of sexually naïve rats by β-sitosterol and $\alpha-\beta$-amyrin acetate isolated from the hexane extract of Mondia whitei, *Asian Pacific Journal of Tropical Biomedicine*, Volume 2, Issue 3, Supplement, 2012, Pages S1266-S1269.

Patel et al., 1999, Biological aspects of reactive nitrogen species, *Biochim. Biophys. Acta.*, 1411, pp.385-400.

Reiter, R. J., Tan D. X. & Burkhardt, S., 2002, Reactive oxygen and nitrogen species and celluar and organismal decline: Amelioration with melatonin, *Mech. of ageing Dev.*, 123, pp.1007-1019.

Rabe S.Z.T., Mahmoudi M. & Emami S.A., 2011, Determination of anti-inflammatory activity of terpenoide fractions of some Artemisia species from Iran, *Clinical biochemistry*, 44(13), pp.S327-S328.

Riadh Ksouri, et al., 2012, Medicinal halophytes: potent source of health promoting biomolecules with medical, *Nutraceutical and food applications.* 32(4), pp.289-326.

Szakiel A1, Pączkowski C, Koivuniemi H & Huttunen S., 2012, Comparison of the triterpenoid content of berries and leaves of lingonberry Vaccinium vitis-idaea from Finland and Poland, *J Agric Food Chem*, 16;60(19), pp.4994-5002.

Seo, Y. et al., 2004 Peroxynitrite scavenging constituents from the brown alga *Sargassum thunbergii*, *Biotechnol. Bioprocess Eng*, 9, pp.212-216

Tsao, L. et al., 2005, Inhibition of lipopolysaccharide-induced expression of inducible nitric oxide synthase by phenolic (3E)-4-(2-hydroxyphenyl)but -3-en-2-one in RAW 264.7 macrophages, *Biochem. Pharmacol*, 70, pp.618-626.

Tadahiro Yahagi, Naoyuki Yakura, Keiichi Matsuzaki & Susumu Kitanaka, 2014, Inhibitory effect of chemical constituents from *Artemisia scoparia* Waldst. et Kit. on triglyceride accumulation in 3T3-L1 cells and nitric oxide production in RAW 264.7 cells, *Journal of Natural Medicines*, 68(2), pp.414-420.

Virag Wagenen, B. C., Huddleston, J and Cardellina, J. H., 1988, Native american food and medicinal plants, 8 water-soluble constituents of *Lomatium Dissectum*, *j. Nat. Prod.*, 51, pp.136-141.

Wang Z.Q., Zhang X.H., Yu Y., 2013, *Artemisia scoparia* extract attenuates non-alcoholic fatty liver disease in diet-induced obesity mice by enhancing hepatic insulin and AMPK signaling independently of FGF21 pathway, Metabolism : clinical and experimental, 62(9), pp.1239-1249.

Yoon W. J. et al., 2006, Anti-oxidant Activities and Anti-inflammatory Effects on Artemisia scoparia, *생약학회지*, 37(4), pp.235-240.

You Ah Kiim, Hee Jung Lee & Youngwan Seo, 2003. Screening on Radical Scavenging Activity of Salt Marsh Plants, *Korean Society for Biotechnology and Bioengineering Journal* 생물공학의 동향(XII), 11, pp.673-675.

Zou, Y., A.R. Kim, J.E. Kim, J.S. Choi, and H.Y. Chung, 2002, Peroxynitrite scavenging activity of sinapic acid (3,5-dimethoxyl-4-hydroxycinnamic acid) isolated from Brassica juncea, *J. Agric. Food Chem.*, 50, 5884-5890.

Appendix

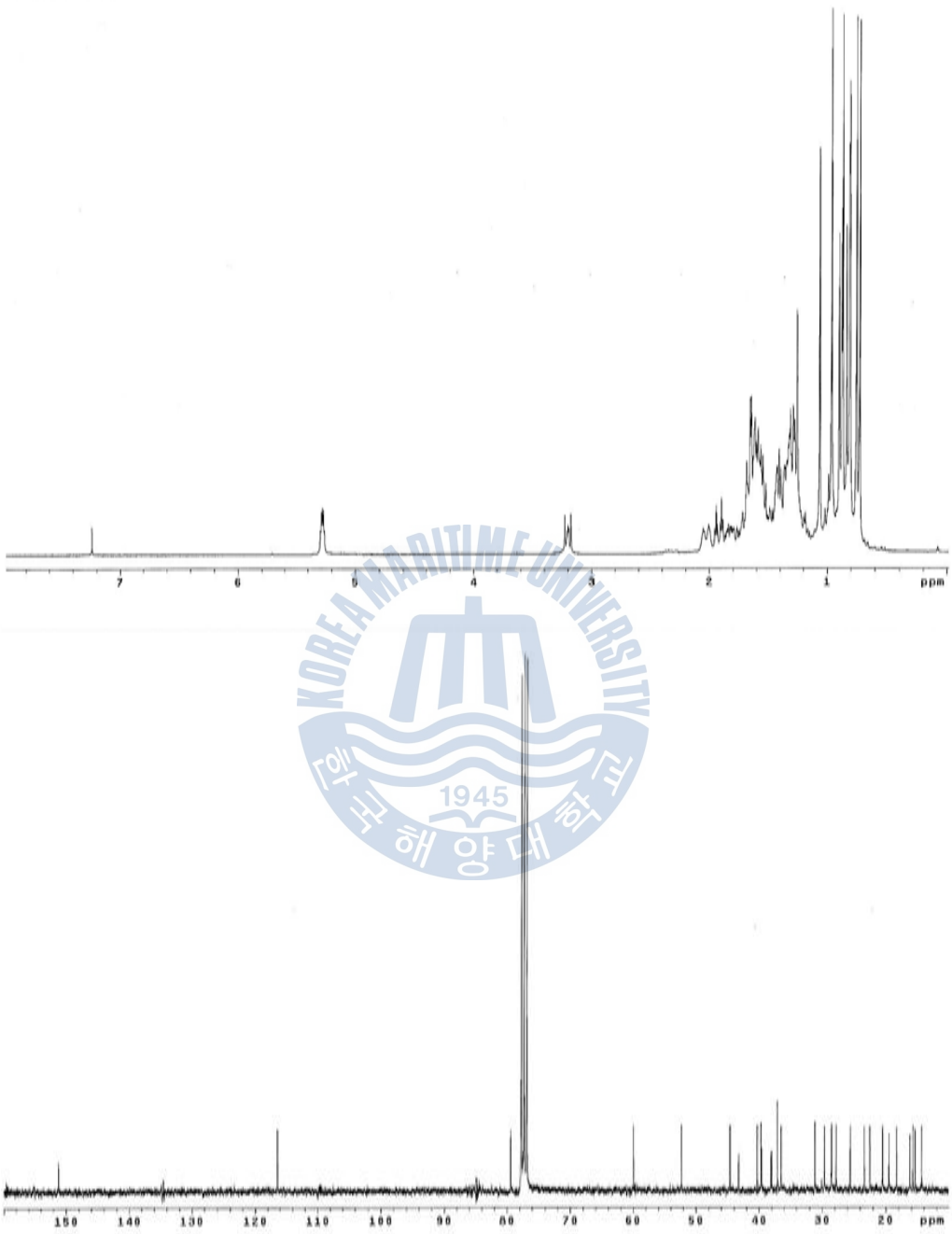

Figure 14. ^{1}H and ^{13}C spectrum of compound **1** isolated from *Artemisia scoparia* in $CDCl_3$.

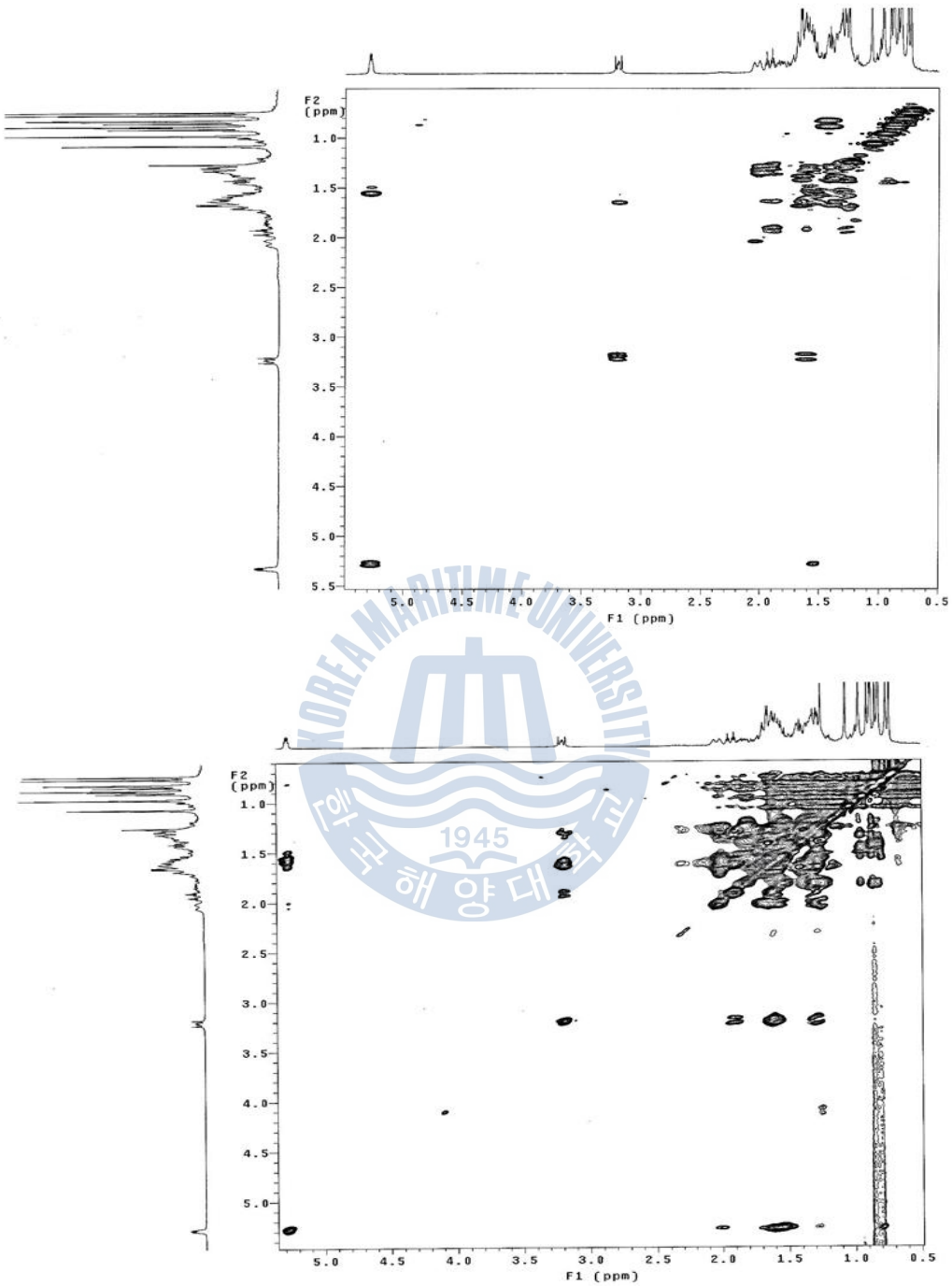

Figure 15. ^{1}H COSY and TOCSY spectrum of compound **1** isolated from *Artemisia scoparia* in $CDCl_3$.

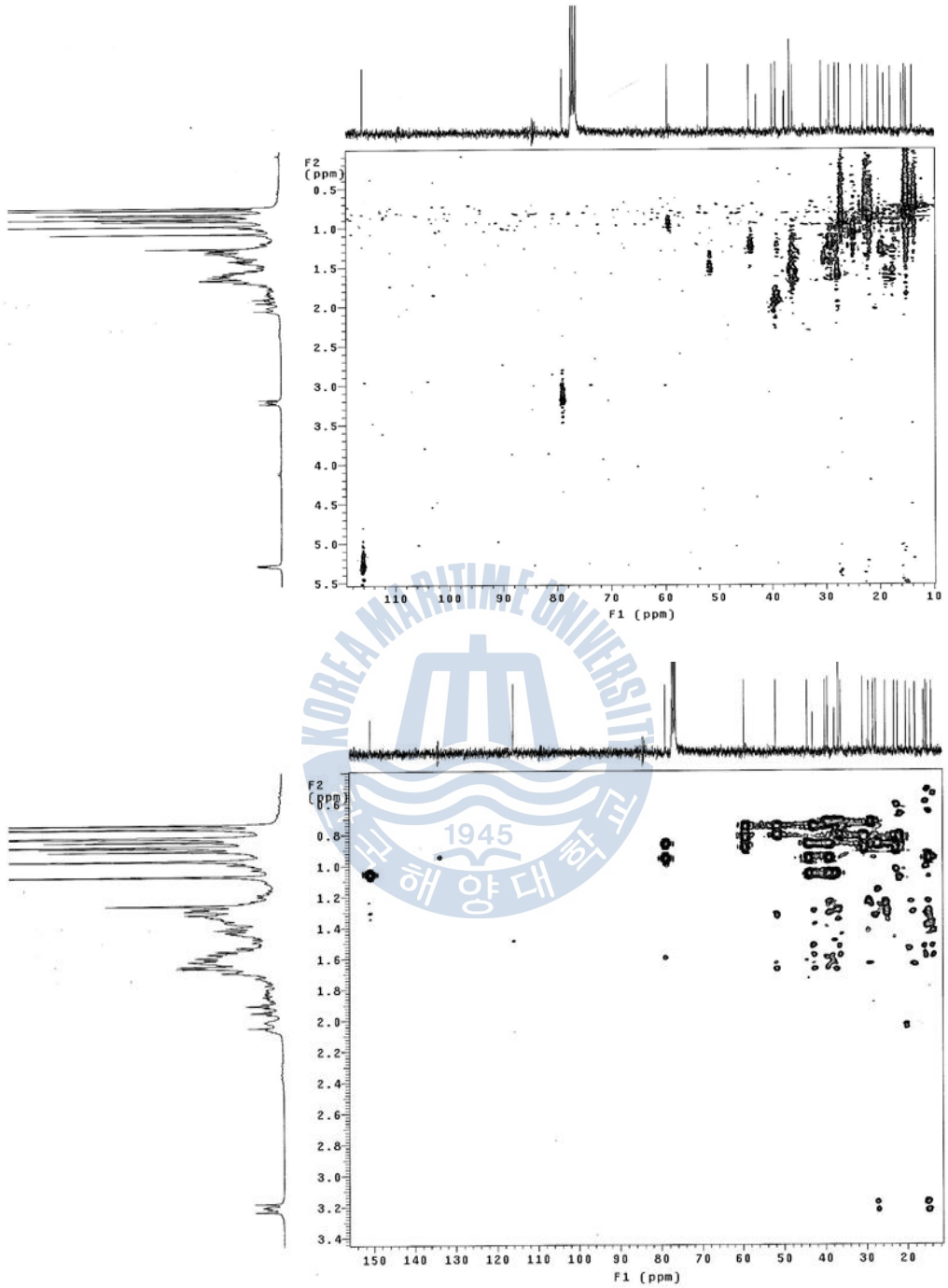

Figure 16. gHMQC and gHMBC spectrum of compound **1** isolated from *Artemisia scoparia* in $CDCl_3$.

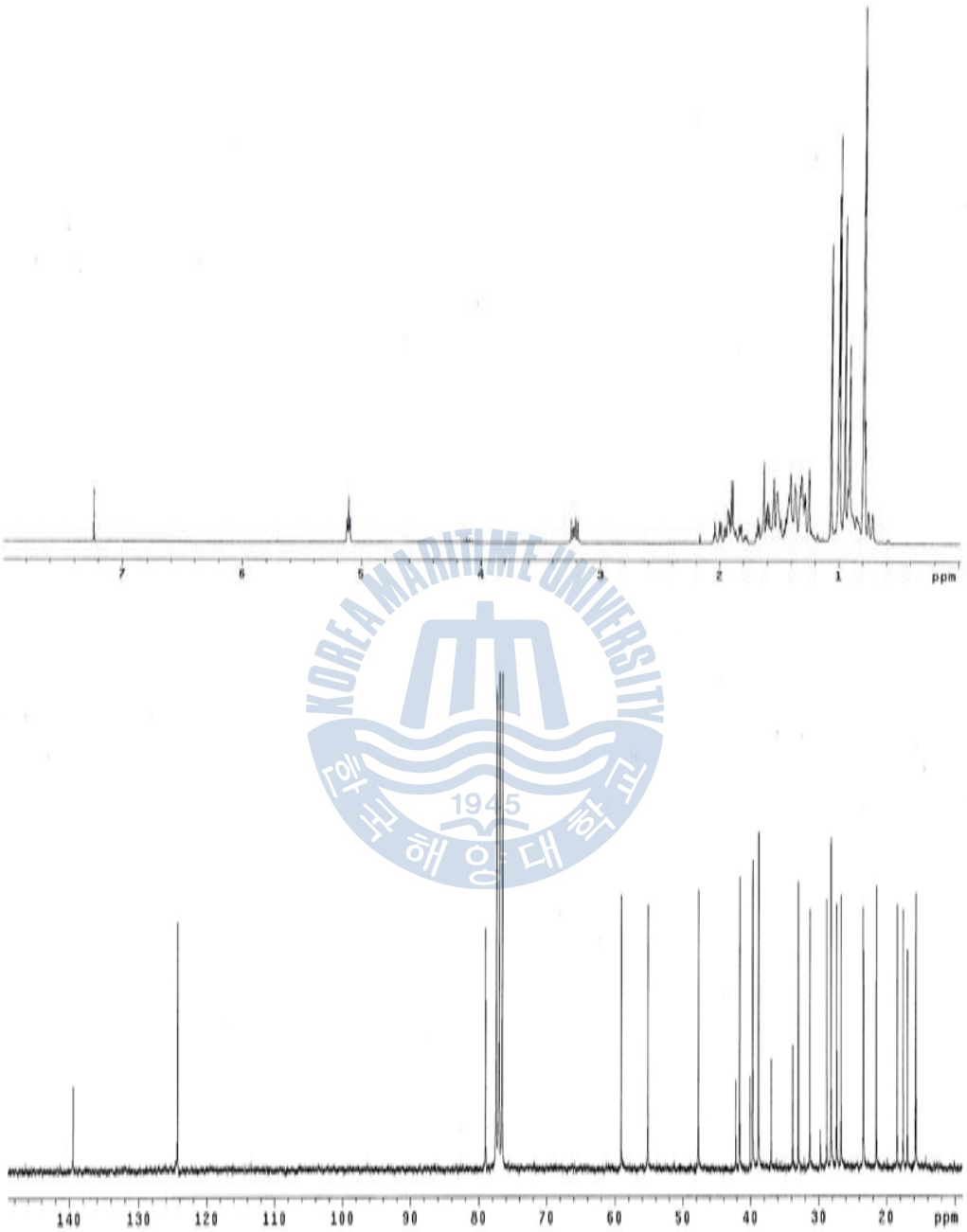

Figure 17. ^{1}H and ^{13}C spectrum of compound **2** isolated from *Artemisia scoparia* in $CDCl_3$.

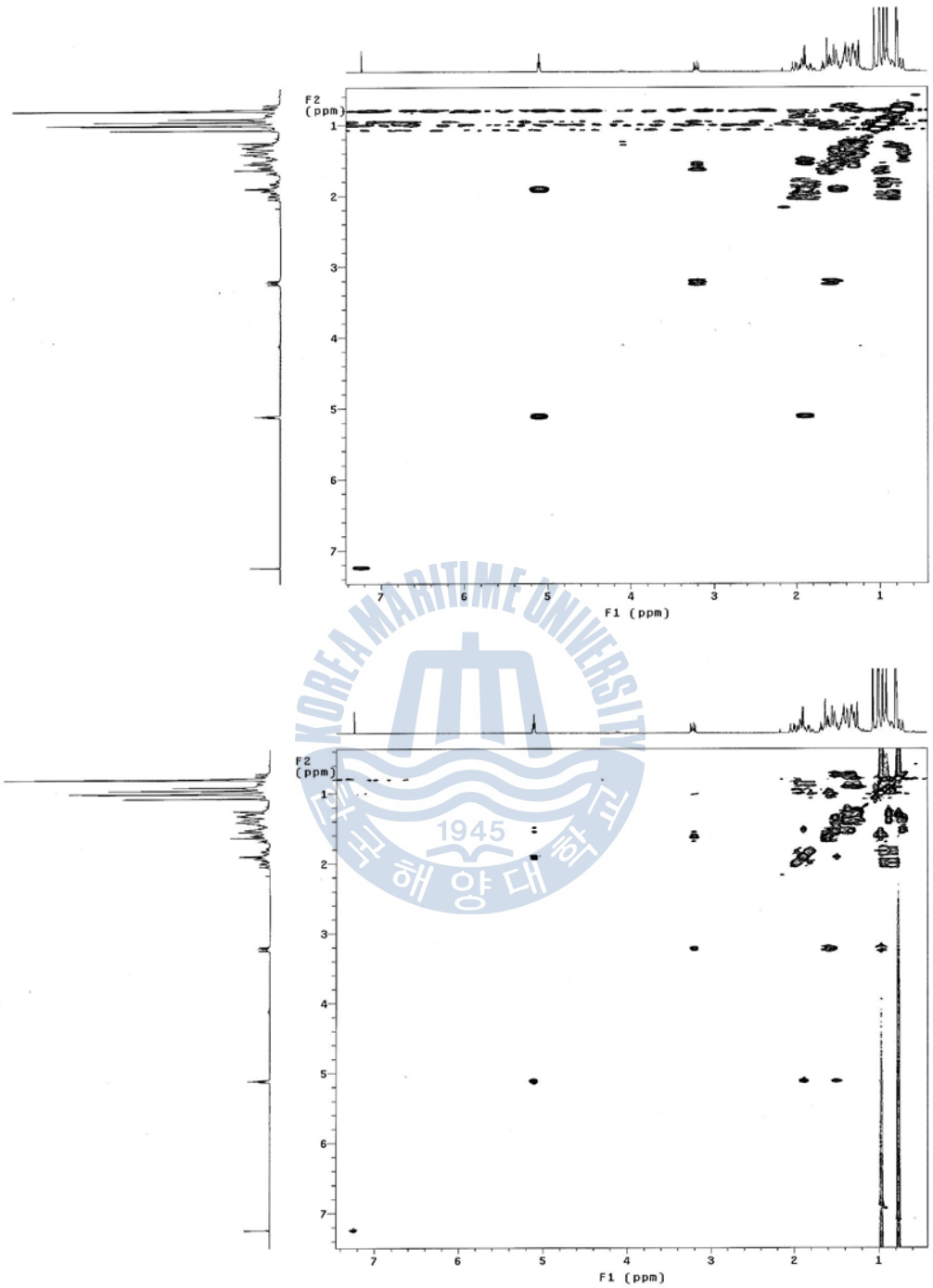

Figure 18. ^{1}H COSY and TOCSY spectrum of compound **2** isolated from *Artemisia scoparia* in $CDCl_3$.

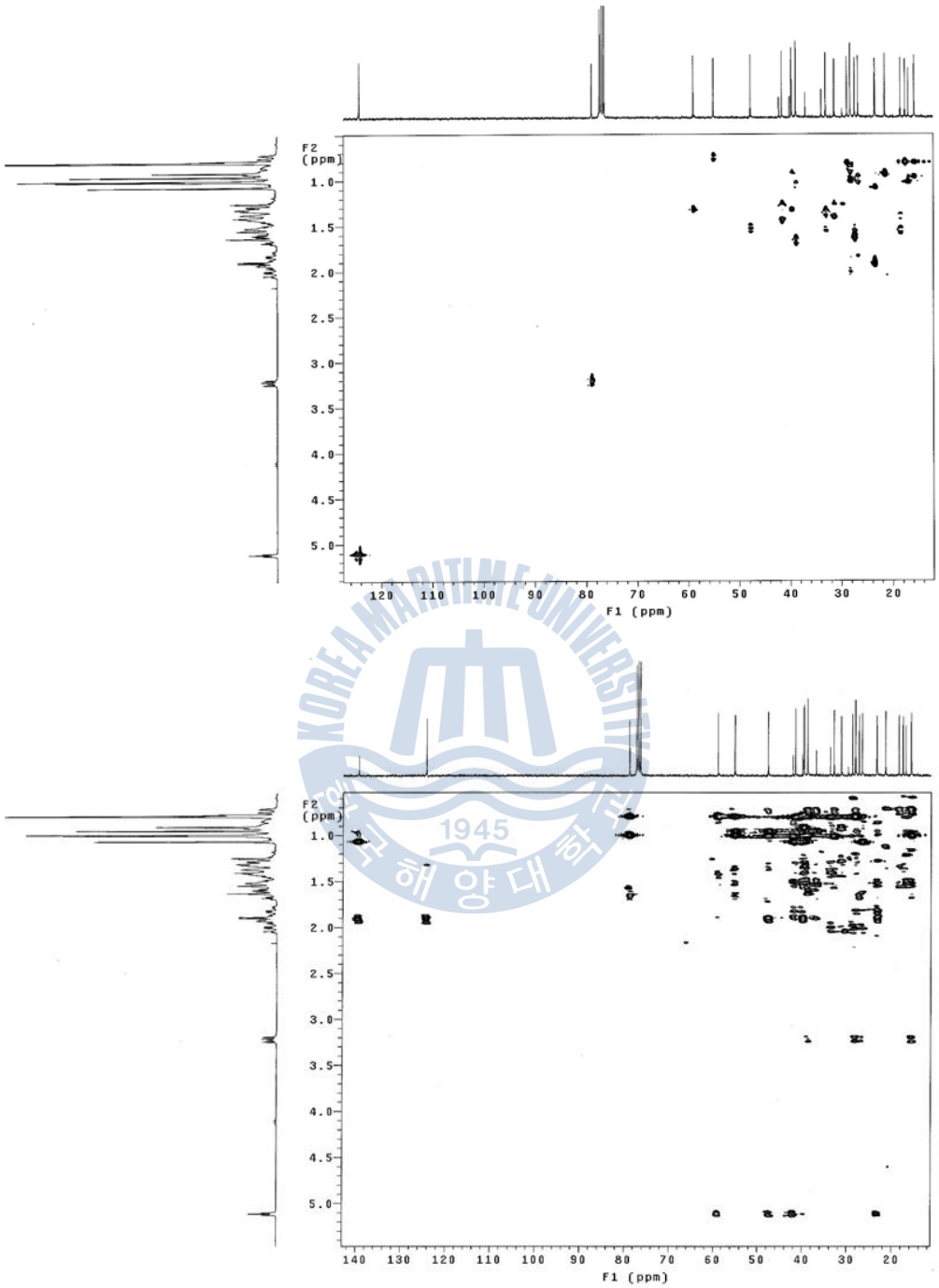

Figure 19. gHMQC and gHMBC spectrum of compound **2** isolated from *Artemisia scoparia* in $CDCl_3$.

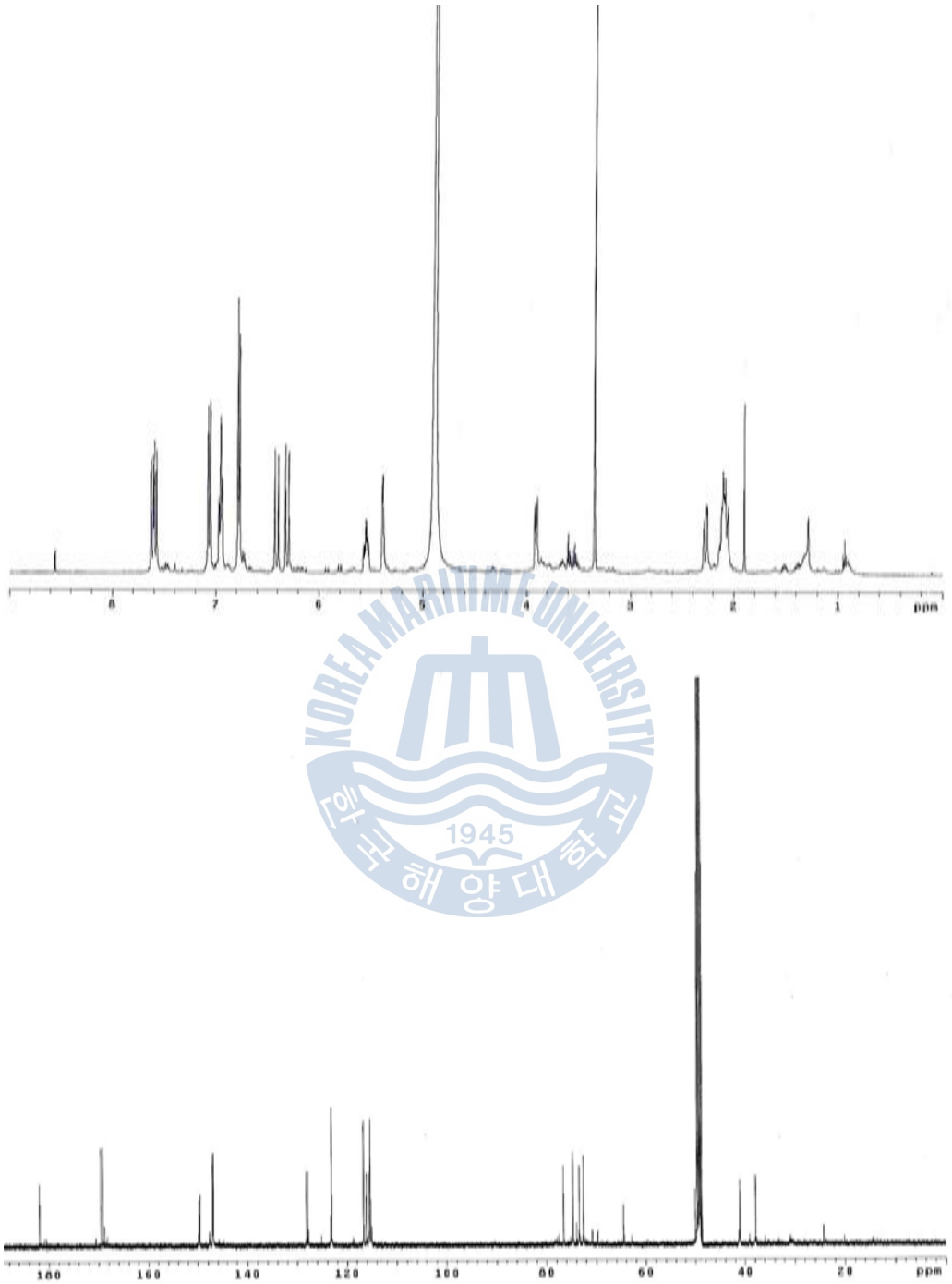

Figure 20. ^{1}H and ^{13}C spectrum of compound **3** isolated from *Artemisia scoparia* in $CDCl_3$.

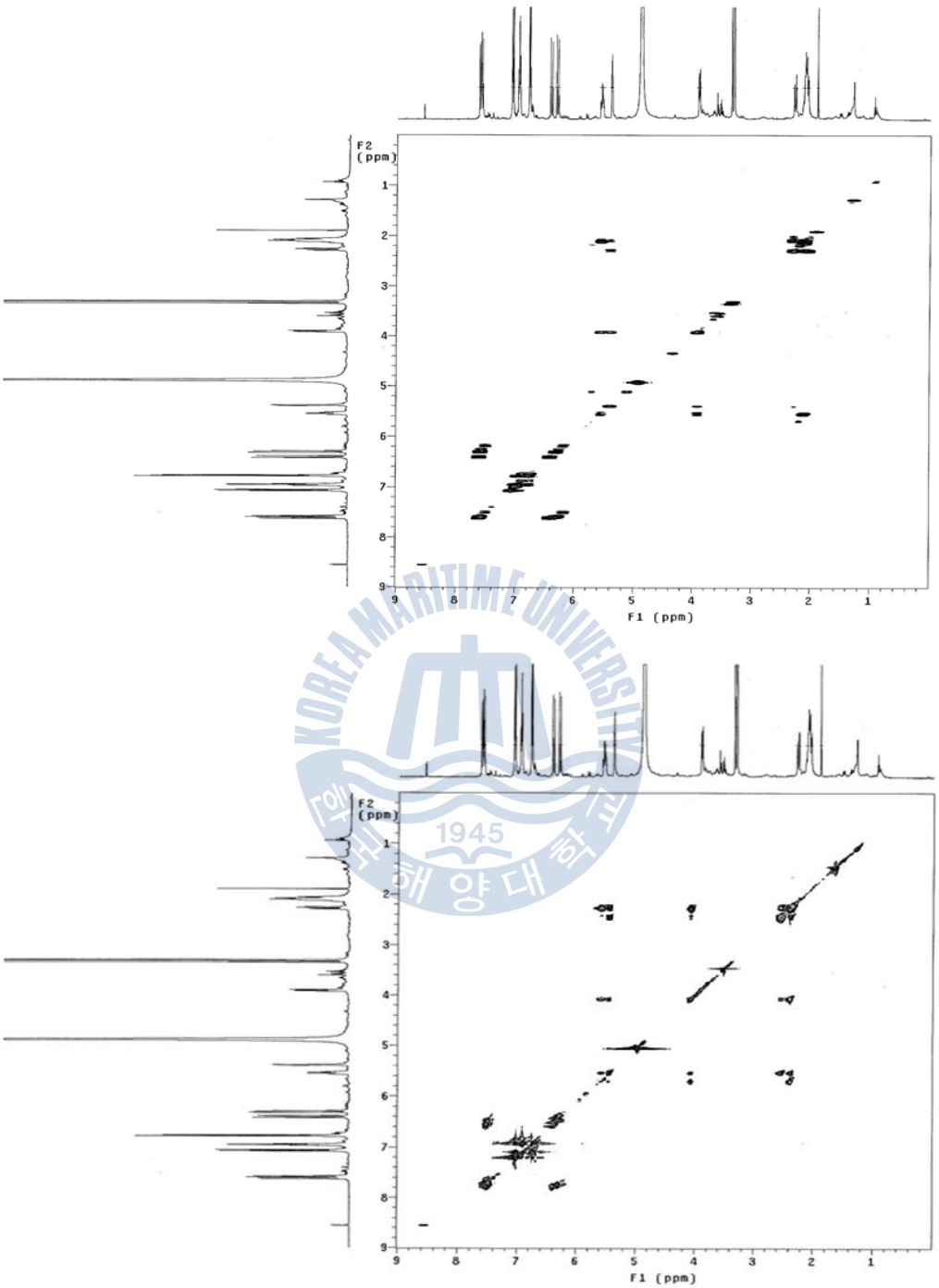

Figure 21. ^{1}H COSY and TOCSY spectrum of compound **3** isolated from *Artemisia scoparia* in $CDCl_3$.

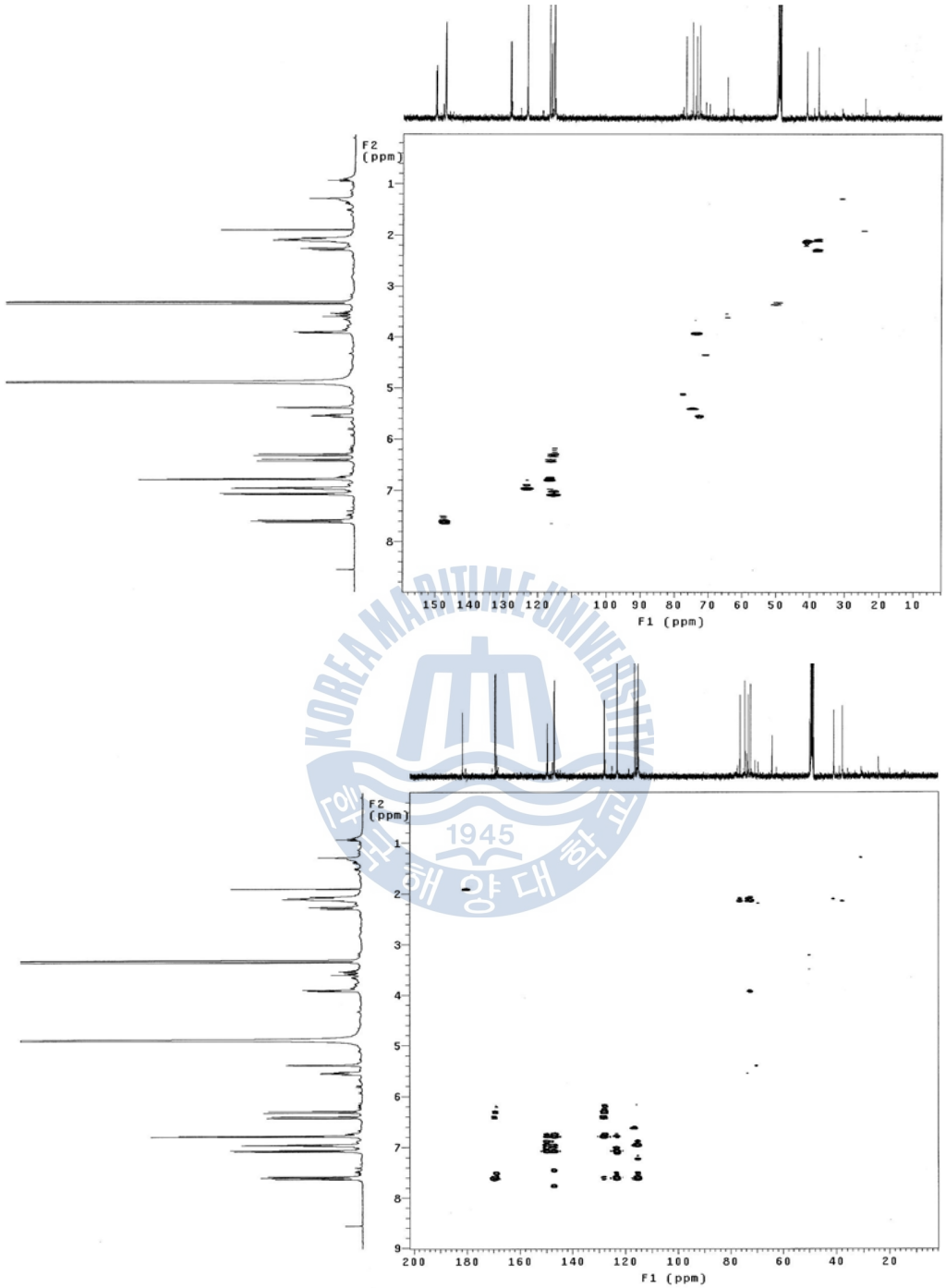

Figure 22. gHMQC and gHMBC spectrum of compound **3** isolated from *Artemisia scoparia* in $CDCl_3$.

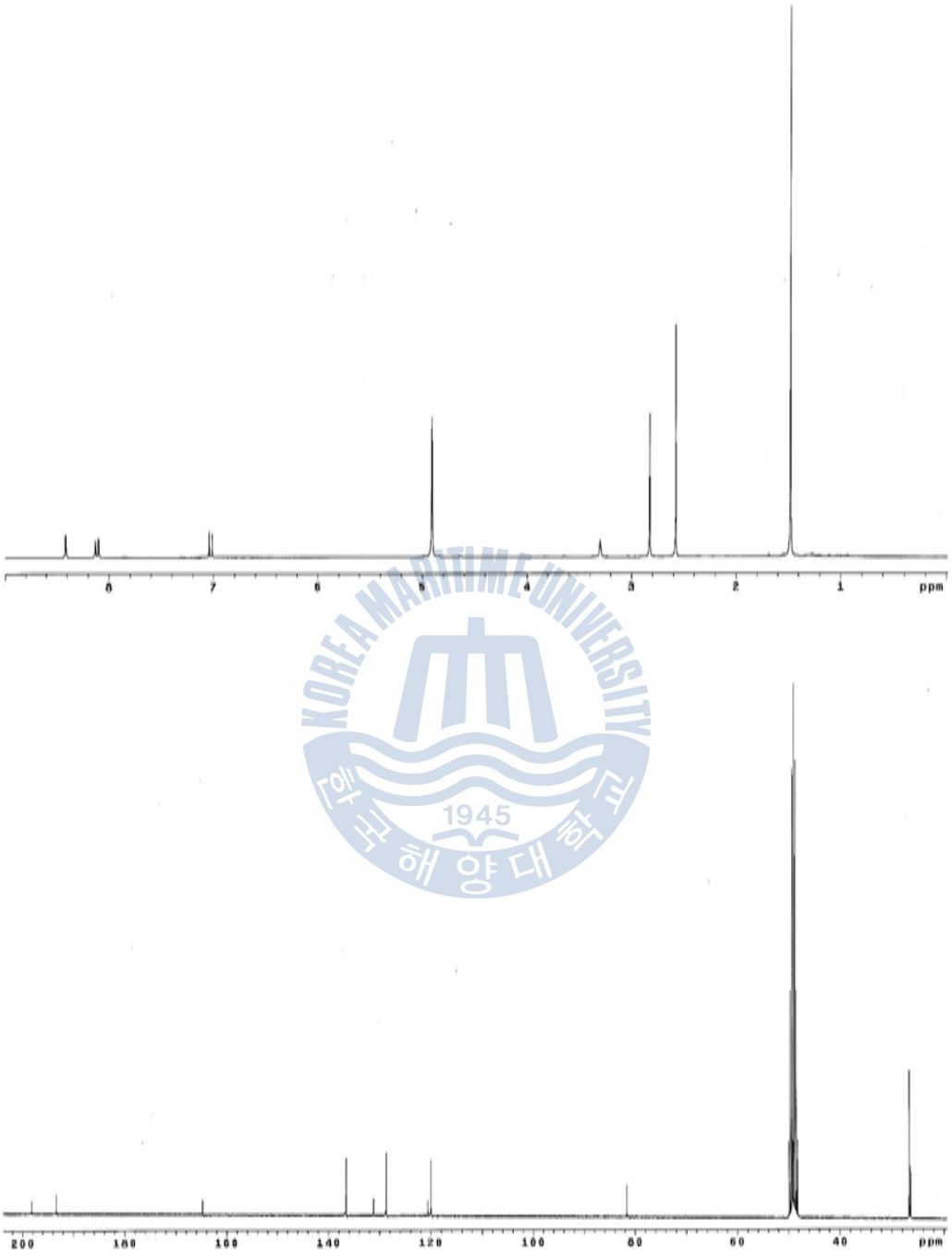

Figure 23. ^{1}H and ^{13}C spectrum of compound **4** isolated from *Artemisia scoparia* in $CDCl_3$.

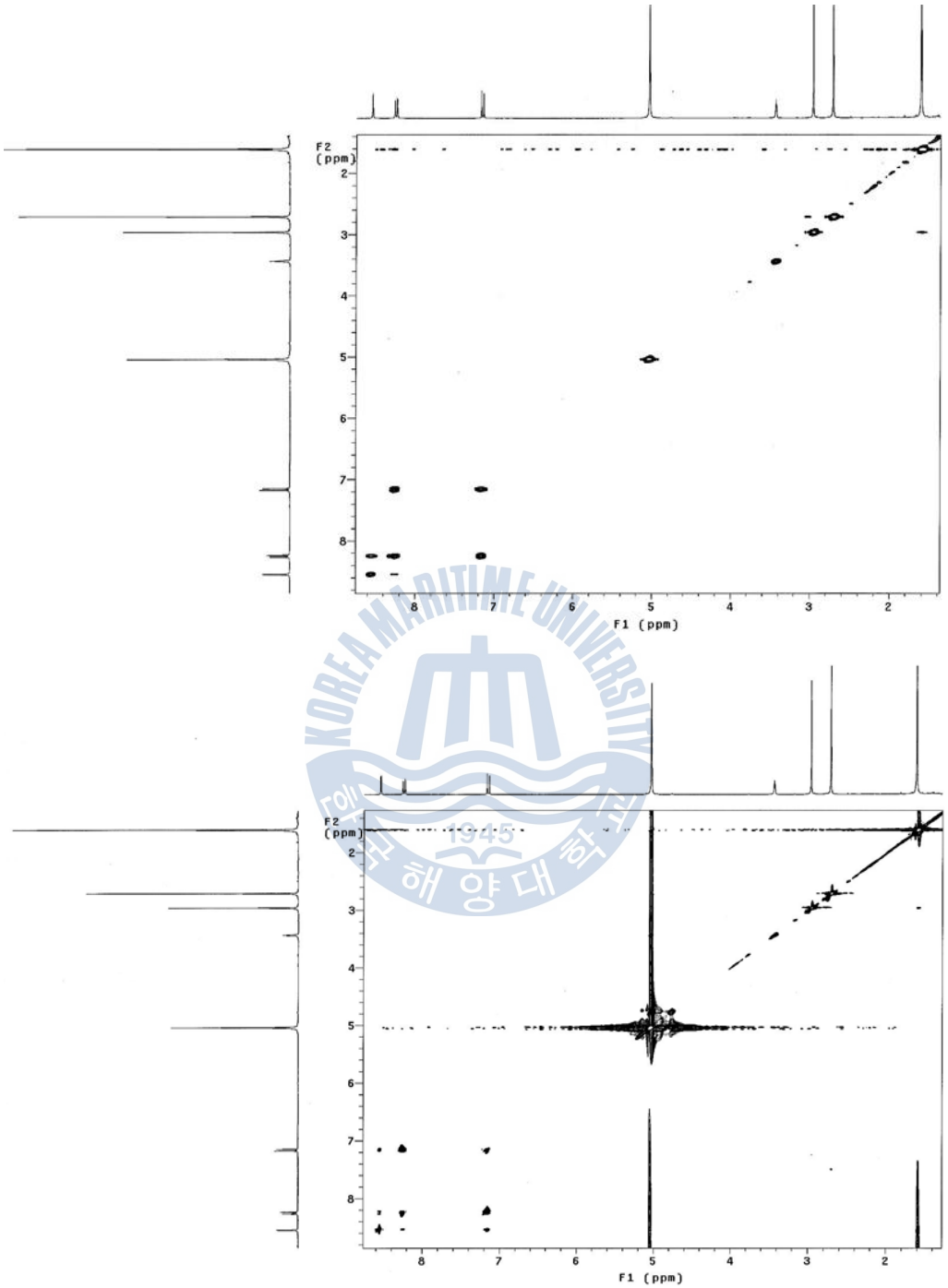

Figure 24. ^{1}H COSY and TOCSY spectrum of compound **4** isolated from *Artemisia scoparia* in $CDCl_3$.

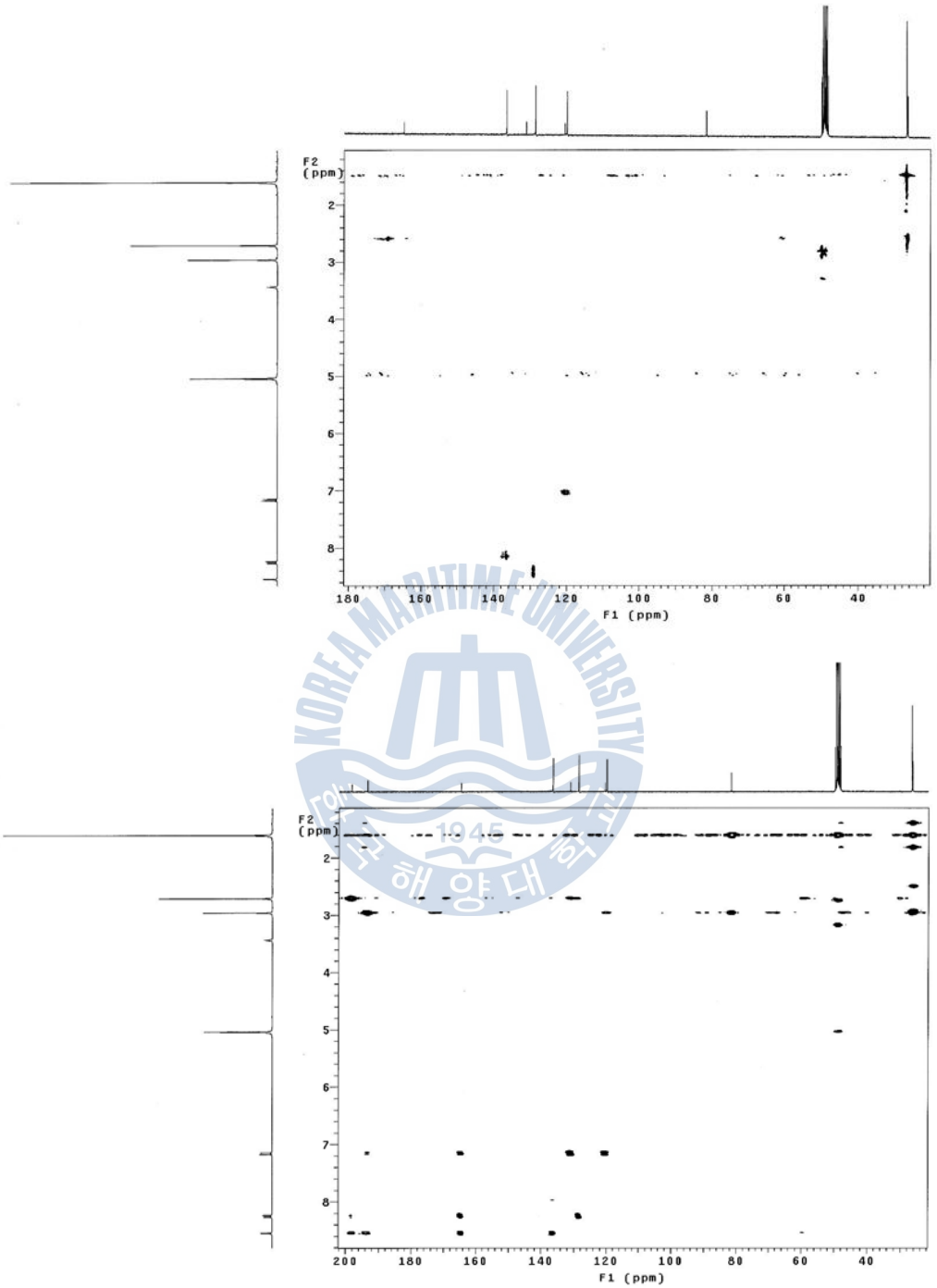

Figure 25. gHMQC and gHMBC spectrum of compound **4** isolated from *Artemisia scoparia* in $CDCl_3$.

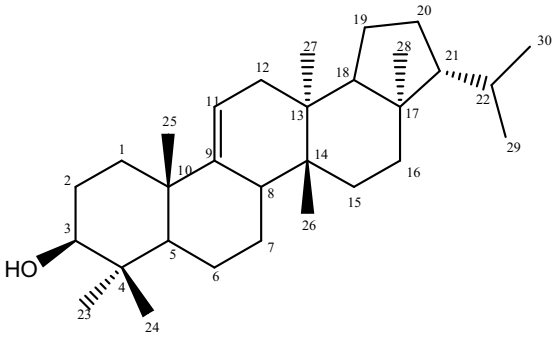

Compound **1**

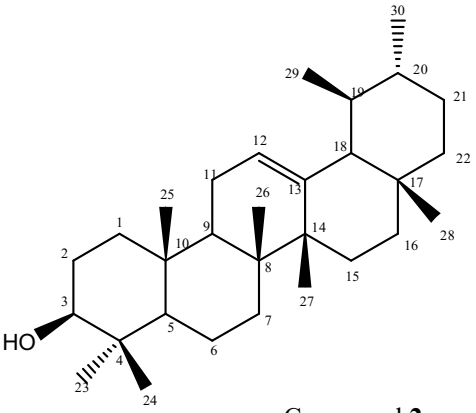

Compound **2**

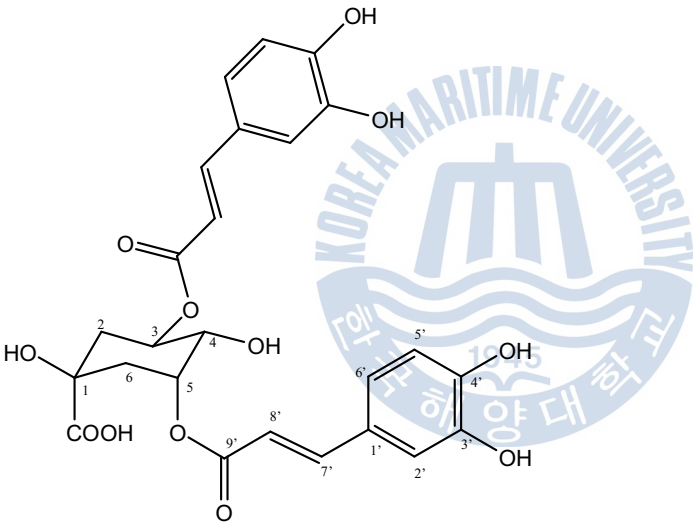

Compound **3**

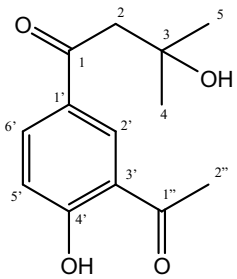

Compound **4**

Figure 26. Chemical structure of compounds **1-4** from *Artemisia scoparia*